Tunneling versus sequential long-range electron transfer: Analogy with pump–probe spectroscopy

Yuming Hu and Shaul Mukamel[a)]
University of Rochester, Chemistry Department, Rochester, New York 14627

(Received 21 July 1989; accepted 18 August 1989)

The interplay between the sequential and the superexchange (tunneling) mechanisms for electron transfer in condensed phases is studied by formulating the problem using the density matrix. The sequential mechanism proceeds via populations of intermediate electronic states (diagonal density matrix elements) whereas the superexchange proceeds through coherences (off diagonal density matrix elements). The present formulation establishes a complete formal analogy between these mechanisms and the incoherent and the coherent pathways in nonlinear optical measurements, in particular, pump–probe spectroscopy.

I. INTRODUCTION

Many important chemical, biological, and solid-state processes involve the transfer of charges (electrons or holes) over long distances (>10 Å), where a direct "through space" coupling between the donor and the acceptor is very small.[1–4] The direct exchange coupling for electron transfer decreases exponentially with the distance between sites $\sim\exp(-R/\ell)$ with a characteristic length ℓ varying between 0.8–1.3 Å.[2,3] It is then likely that sites other than the donor and the acceptor could participate in these processes. One possible mechanism for the electron transfer is a direct *tunneling* mechanism whereby the electron tunnels from the donor to the acceptor without spending any appreciable amount of time at intermediate sites. The other sites play a passive role in the process by contributing to the tunneling matrix element. This is the essence of the superexchange model developed in the theory of magnetism by Anderson[5] and first applied to electron transfer by McConnel.[6,7] The superexchange model of a particle or a quasiparticle (spin, exciton) assumes that the intermediate site energies are sufficiently high, so that the process involves only a virtual excitation of these sites. In intramolecular electron transfer this is referred to as "through bond" coupling.[3,7] Alternatively we can envision a *sequential* transfer mechanism which proceeds through a succession of incoherent hops among closely lying sites. The mechanism requires the availability of sites whose energies are within a few k_BT of the donor energy, since the process is thermally activated.[8–10] If we envision a system with high-intermediate site energies, the superexchange mechanism will be dominant. As these energies are lowered, there is an interesting interplay between both mechanisms. In this article we develop a systematic method for calculating electron transfer (ET) and transport in a multicenter system coupled to a thermal bath. By formulating the problem using the density matrix in Liouville space[11,12] we carry out the averaging over the solvent degrees of freedom and identify the distinct Liouville space pathways which are responsible for both mechanisms. This way we obtain both mechanisms as limiting cases of the same unified theory. Explicit expressions are derived for a three-site system when the solvent timescale is slow (static limit) or fast (homogeneous dephasing). The evaluation of the rate matrix in the static limit is the main accomplishment of this article. The present theory holds for any values of the energy parameters ΔG^0_{jk} and the reorganization energy parameters λ_j and can therefore be used to explore the relative contribution of the superexchange and the sequential electron transfer. The fast fluctuation (homogeneous dephasing) limit is less realistic for typical ET processes than the static limit. It is an infinite temperature approximation[11,13,14] which cannot reproduce the correct detailed balance condition. Nevertheless, since it is exactly solvable to infinite order in the nonadiabatic coupling, its analysis provides a useful insight on the dynamics of ET processes.

The problem of superexchange versus sequential mechanisms for electron transfer is intimately related to the dynamics of nonlinear optical line shapes.[15] The expression for the nonadiabatic rate using the Fermi golden rule and the superexchange coupling matrix element [Eq. (5.3)] is the analog of the Kramers–Heisenberg expression for Raman spectroscopy.[16] There, too, the system evolves from the initial to the final state via an intermediate off-resonance state. The analogy is not limited however to ordinary Raman and off-resonance situations. More generally any optical transition can proceed coherently or sequentially. The transition from Raman to fluorescence spectra as the optical frequencies are resonantly tuned, or the dephasing rate is increased, is completely analogous to the transition from the superexchange to the sequential mechanisms.[16] There is a whole family of nonlinear optical spectroscopies related to four-wave mixing and the nonlinear susceptibility $\chi^{(3)}$, whose theory closely resembles that of the electron transfer. We have drawn this analogy previously for the simpler two-site problem.[17] In this article we show that the dynamics of two photon transitions and in particular pump-probe spectroscopy[18–20] is formally identical to the problem of electron transfer in a three-site system.

The remainder of this article is organized as follows. In Sec. II we derive a formal expression for the electron transfer rate in an N-site system coupled to a thermal bath. The rate expressions are formally exact, and expanded as a power series in the coupling constant V_{jk}. In Sec. III we truncate the expansion to fourth order for a three-site system, and

[a)] Camille and Henry Dreyfus Teacher/Scholar.

 0021-9606/89/236973-16$02.10 © 1989 American Institute of Physics

Downloaded 21 Jun 2002 to 128.151.176.185. Redistribution subject to AIP license or copyright, see http://ojps.aip.org/jcpo/jcpcr.jsp

express the rate matrix in terms of solvent correlation functions. In Sec. IV we evaluate these correlation functions in the limit of slow solvent fluctuations (the static limit) and obtain the complete rate matrix for the three-site system. These rate expressions are used in Sec. V to investigate the relative contribution of the superexchange and the sequential electron transfer using parameters typical for the photosynthetic reaction center. In Sec. VI the electron transfer process for a three-site system is analyzed in the fast fluctuation (homogeneous dephasing) limit. Finally, in Sec. VII we establish the connection with stationary and femtosecond pump–probe spectroscopy. Important technical details are given in Appendices A–E.

II. FORMAL EXPRESSION FOR THE ELECTRON TRANSFER RATE

We consider an electron transfer (ET) system in which the electron has N accessible sites, embedded in a medium (solvent). We denote by $|j\rangle$ the state whereby the electron resides on the jth site $j=1,2,...,N$. The j and k sites are coupled by an exchange nonadiabatic coupling V_{jk}, which decreased exponentially with the intersite separation. We assume that this coupling is not affected substantially by the dynamical behavior of the solvent and thus does not depend on the solvent coordinates. The interaction of the solvent with the system will depend on the electronic state $|j\rangle$. We denote the solvent adiabatic Hamiltonian in the state $|j\rangle$ by $H_j(Q)$, where Q denotes the nuclear degrees of freedom of the solvent. The total model Hamiltonian for the system and solvent is

$$H=H_0+H', \tag{2.1}$$

where

$$H_0=\sum_{j=1}^{N}|j\rangle H_j(Q)\langle j|, \tag{2.2a}$$

$$H'=\sum_{\substack{j,k=1\\ j\neq k}}^{N}V_{jk}|j\rangle\langle k|. \tag{2.2b}$$

We will set throughout this article $\hbar=1$, except in the final expressions for the rate, where $\hbar$ will be explicitly included. The total density matrix $\rho(t)$ of the ET system and the solvent satisfies the Liouville equation

$$d\rho(t)/dt=-i[H,\rho(t)]\equiv -iL\rho(t), \tag{2.3}$$

where the Liouville space operators L_0, L', and L are defined by their action on an ordinary operator A, i.e.,[16]

$$\begin{aligned} &L_0A\equiv[H_0,A],\\ &L'A\equiv[H',A],\\ &LA\equiv[H,A]. \end{aligned} \tag{2.4}$$

We further introduce the following complete set of system operators

$$A_{jk}=|j\rangle\langle k| \tag{2.5}$$

which satisfy

$$A_{jk}A_{nm}=A_{jm}\delta_{kn}. \tag{2.6}$$

We denote the total trace, and the partial traces over the ET system and over the solvent by Tr, Tr^e, and Tr^Q, respectively. By definition $\mathrm{Tr}\equiv\mathrm{Tr}^Q\mathrm{Tr}^e$. The population on state $|j\rangle$ at time t is given by

$$p_j(t)=\mathrm{Tr}(A_{jj}\rho)=\mathrm{Tr}^Q\langle j|\rho(t)|j\rangle. \tag{2.7}$$

We now define the projection operator $\hat{P}$ acting on an arbitrary operator B in the Hilbert space of the total ET system and the solvent by[12]

$$\hat{P}B=\sum_j\rho_jA_{jj}\mathrm{Tr}(A_{jj}B) \tag{2.8a}$$

and the complementary projection by

$$\hat{Q}=1-\hat{P}, \tag{2.8b}$$

where ρ_j is the equilibrium solvent density matrix in the sate $|j\rangle$, i.e.,

$$\rho_j=\exp(-H_j/k_BT)/\mathrm{Tr}^Q\{\exp(-H_j/k_BT)\}. \tag{2.9}$$

We assume that at $t=0$ the population in state $|j\rangle$ is $p_j(0)$ and the solvent is in thermal equilibrium, i.e.,

$$\rho(0)=\sum_{j=1}^{N}p_j(0)A_{jj}\rho_j. \tag{2.10}$$

One can easily show, using Eqs. (2.8)–(2.10)

$$\begin{aligned} &\hat{P}\rho(0)=\rho(0),\\ &L_0\hat{P}=\hat{P}L_0=0,\\ &\hat{P}L_1\hat{P}=0. \end{aligned} \tag{2.11}$$

Making use of standard projection operator techniques,[21] we can derive a generalized master equation for the populations

$$d\mathbf{P}/dt=\int_0^t\mathbf{K}(t-\tau)\mathbf{P}(\tau)\,d\tau, \tag{2.12}$$

where $\mathbf{P}$ is an N-dimensional vector with components $p_j(t)$ and $\mathbf{K}(t)$ is an $N\times N$ generalized rate matrix, with matrix elements $K_{jk}(t)$. We further introduce the Laplace transform of $\mathbf{K}(t)$, i.e.,

$$K_{jk}(s)=\int_0^\infty dt\exp(-st)K_{jk}(t).$$

The exact formal expression for $K_{jk}(s)$ is

$$K_{jk}(s)=-\mathrm{Tr}\left[A_{jj}\frac{1}{1+L'G_0L'G_0\hat{Q}}L'G_0L'A_{kk}\rho_k\right] \tag{2.13a}$$

with the Green function

$$G_0\equiv 1/(s+iL_0). \tag{2.13b}$$

$K_{jk}(s)$ can be expanded in a power series in L', i.e.,

$$K_{jk}(s)=\sum_{n=1}^{\infty}(-1)^nK_{jk}^{(2n)}(s), \tag{2.14a}$$

where

$$K_{jk}^{(2n)}(s)=\mathrm{Tr}[A_{jj}(L'G_0L'G_0\hat{Q})^{n-1}L'G_0L'A_{kk}\rho_k]. \tag{2.14b}$$

It will be useful to eliminate the complementary projection $\hat{Q}$ in $K_{jk}^{(2n)}$ and express $K_{jk}^{(2n)}$ in terms of the matrix $\mathbf{T}^{(2m)}$, whose elements $T_{jk}^{(2m)}$ are defined by

$$T_{jk}^{(2m)}(s)=\mathrm{Tr}[A_{jj}(L'G_0L'G_0)^{m-1}L'G_0L'A_{kk}\rho_k]. \tag{2.15}$$

Downloaded 21 Jun 2002 to 128.151.176.185. Redistribution subject to AIP license or copyright, see http://ojps.aip.org/jcpo/jcpcr.jsp

Following the derivation of Appendix A in Ref. [12a], we have the recursion relation:

$$\mathbf{K}^{(2n)}(s) = \mathbf{T}^{(2n)}(s) - \frac{1}{s}\sum_{m=0}^{n-2} \mathbf{K}^{2(n-m-1)}(s)\mathbf{T}^{2(m+1)}(s) , \quad n = 2,3,\ldots . \tag{2.16}$$

Equations (2.14)–(2.16) constitute the basis for calculating the electron transfer rate $K_{jk}(s)$. We first calculate $\mathbf{T}^{(2n)}$ to the desired order and then calculate the frequency dependent rate constant $\mathbf{K}^{(2n)}$ using the recursion relation [Eq. (2.16)]. Note that $\mathbf{K}^{(2)} = \mathbf{T}^{(2)}$ and in general $\mathbf{K}^{(2n)}$ may be expressed in terms of $\mathbf{T}^{(2m)}$ with $m \leqslant n$. In many cases, the ET process is much slower than the dynamics of the solvent degrees of freedom. In that case the system satisfies an ordinary rate equation where the ordinary rate matrix is $\mathbf{K} \equiv \mathbf{K}(s=0)$, i.e.,

$$d\mathbf{P}/dt = \mathbf{K}\mathbf{P} . \tag{2.17}$$

It should be noted that the divergent $1/s$ factor in Eq. (2.16) will not cause any difficulty in that limit since it is cancelled by other terms so that $\mathbf{K}^{(2n)}(s=0)$ is well behaved.[12] The remainder of this article will focus on analyzing the ET rate for a three-site system.

III. GENERALIZED RATE MATRIX FOR A THREE-SITE SYSTEM

We shall specialize to a three-site system, which is the simplest model showing the interplay between tunneling and sequential electron transfer. The Hamiltonian Eq. (2.1) thus becomes

$$H = \sum_{j=1}^{3} |j\rangle H_j(Q)\langle j| + V_{12}(|1\rangle\langle 2| + |2\rangle\langle 1|) + V_{23}(|2\rangle\langle 3| + |3\rangle\langle 2|) . \tag{3.1}$$

When the nonadiabatic coupling V_{jk} is sufficiently weak, we can truncate the expansion [Eq. (2.14a)] to fourth order in V_{jk}, which is the lowest order contributing to $K_{31}(s)$ and $K_{13}(s)$. We thus have

$$K_{nm}(s) \cong K^{(2)}_{nm}(s) + K^{(4)}_{nm}(s) , \tag{3.2}$$

$$K^{(2)}_{nm}(s) = T^{(2)}_{nm}(s) , \tag{3.3a}$$

$$K^{(4)}_{nm}(s) = T^{(4)}_{nm}(s) - (1/s)\sum_{j=1}^{3} T^{(2)}_{nj}(s)T^{(2)}_{jm}(s) , \tag{3.3b}$$

where

$$T^{(2)}_{nm}(s) = \mathrm{Tr}(A_{nn}L'G_0L'A_{mm}\rho_m) , \tag{3.4a}$$

$$T^{(4)}_{nm}(s) = \mathrm{Tr}(A_{nn}L'G_0L'G_0L'G_0L'A_{mm}\rho_m) . \tag{3.4b}$$

When the Green function G_0 acts on A_{nm} it makes it evolve by H_n from the left and by H_m from the right. We shall therefore introduce a new definition of a Green function which acts only on solvent operators

$$\hat{G}_{nm}(t)B \equiv \exp(-iH_n t)B\exp(iH_m t) , \tag{3.5}$$

where B is any solvent operator. In the frequency domain we have

$$G_{nm}(s)B \equiv \int_0^\infty dt \exp(-st)\hat{G}_{nm}(t)B . \tag{3.6}$$

The trace over the electronic states in Eqs. (3.4) can be easily evaluated since the Green function G_0 is diagonal in the site representation. The bookkeeping of the various terms contributing to $T^{(4)}_{jk}$, $j,k = 1,2,3$ may be visualized using Fig. 1(a). In this figure we show the complete 3×3 density matrix of the system. Each bond represents the nonadiabatic coupling V_{jk}. Since in the Liouville equation [Eq. (2.3)] L' acts as a commutator, it can act either from the left (vertical bond) or from the right (horizontal bond). In order to calculate $T^{(4)}_{31}$ for example, we need to start in 11 and count all the possible 4-bond pathways which lead to 33. A simple inspection of Fig. 1(a) shows that there are six such pathways. Since the paths appear always in complex conjugate

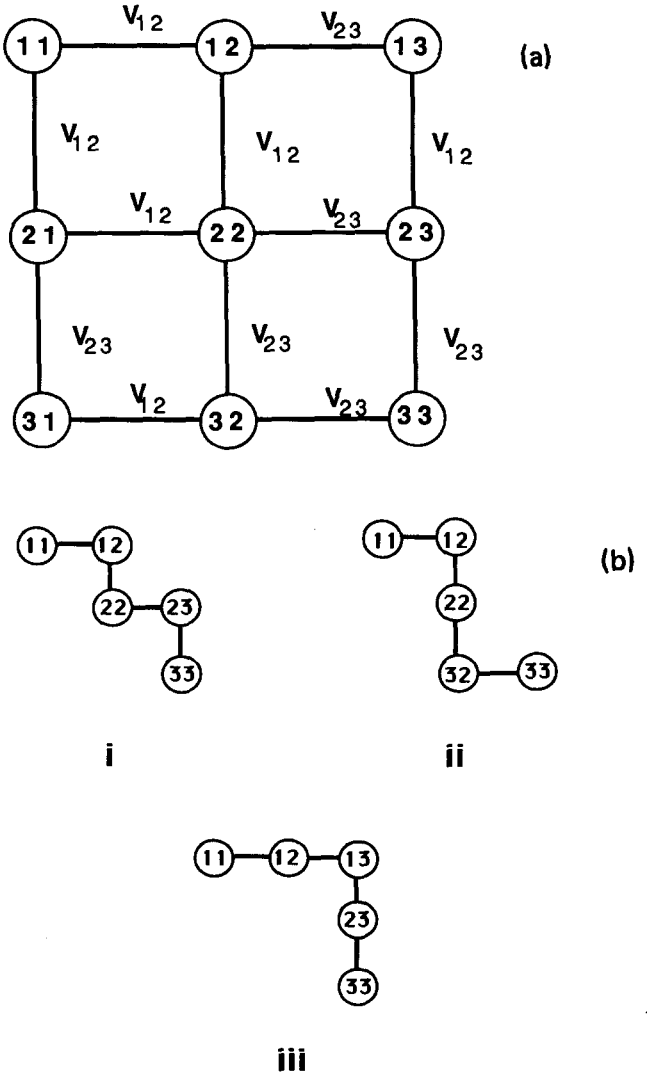

FIG. 1. (a) Liouville-space coupling scheme (Refs. 16 and 17) showing the pathways contributing to the ET rate. Each bond represents a nonadiabatic coupling V_{jk} as indicated (see the text). (b) Liouville-space pathways (Ref. 16) contributing to the rate K_{31} to fourth order in the nonadiabatic coupling. From (a) we see that there are six pathways which lead from 11 to 33 in fourth order. We need to consider only the three pathways shown (the others are their complex conjugates). Pathways (i) and (ii) represent a sequential nonequilibrium process and pathway (iii) is the tunneling (superexchange) term. The three terms in Eq. (3.7) correspond to pathways (i), (ii), and (iii), respectively.

Downloaded 21 Jun 2002 to 128.151.176.185. Redistribution subject to AIP license or copyright, see http://ojps.aip.org/jcpo/jcpcr.jsp

pairs, we only need to consider half of the paths, which are shown in Fig. 1(b). Further description of these type of diagrams was given elsewhere.[16] Apart from the initial 11 and final 33 points on this figure, each path will have three intermediate points. Each intermediate point labelled jk corresponds to a Green function $G_{jk}(s)$. The corresponding expression for $T_{31}^{(4)}(s)$ is

$$T_{31}^{(4)}(s) = 2V_{12}^2 V_{23}^2 \,\mathrm{Re}[\langle G_{23}(s)G_{22}(s)G_{12}(s)\rho_1\rangle + \langle G_{32}(s)G_{22}(s)G_{12}(s)\rho_1\rangle + \langle G_{23}(s)G_{13}(s)G_{12}(s)\rho_1\rangle] , \tag{3.7}$$

where we have used angular brackets $\langle\cdots\rangle$ to denote a trace over the solvent Tr^Q. The three terms in Eq. (3.7) correspond, respectively, to pathways (i), (ii), and (iii) in Fig. 1(b). They can be classified into two types. The first is the paths that start at population 11 and end up at population 33 passing only through coherences (i.e., G_{12}, G_{13}, G_{23}) [path (iii)]. The other type is the paths which pass once through the population 22 [paths (i) and (ii)]. This classification is also valid for all the paths representing the other elements of $T_{jk}^{(4)}(s)$. We shall introduce angular brackets $\langle\cdots\rangle$ with subscripts c or p to represent the paths which pass only through coherences (G_{jk}) with $j\neq k$ and the paths which pass through the population (G_{kk}) once. We shall denote them the coherent and the population pathways, respectively.

$$\langle G_{j'}(s)G_{kh}(s)G_{nm}(s)\rho_r\rangle_c \equiv \langle G_{j'}(s)G_{kh}(s)G_{nm}(s)\rho_r\rangle + \langle G_{'j}(s)G_{hk}(s)G_{mn}(s)\rho_r\rangle , \quad h\neq k , \tag{3.8a}$$

$$\langle G_{j'}(s)G_{kk}(s)G_{nm}(s)\rho_r\rangle_p \equiv \langle [G_{j'}(s)+G_{'j}(s)]G_{kk}(s)[G_{nm}(s)+G_{mn}(s)]\rho_r\rangle - (1/s)\langle [G_{j'}(s)+G_{'j}(s)]\rho_k\rangle \times \langle [G_{nm}(s)+G_{nm}(s)]\rho_r\rangle . \tag{3.8b}$$

These correlation functions have the following symmetries:

$$\langle G_{j'}(s)G_{kh}(s)G_{nm}(s)\rho_r\rangle_c = \langle G_{'j}(s)G_{hk}(s)G_{mn}(s)\rho_r\rangle_c \tag{3.9a}$$

$$\langle G_{j'}(s)G_{kk}(s)G_{nm}(s)\rho_r\rangle_p = \langle G_{'j}(s)G_{kk}(s)G_{nm}(s)\rho_r\rangle_p = \langle G_{j'}(s)G_{kk}(s)G_{mn}(s)\rho_r\rangle_p . \tag{3.9b}$$

The other elements of $T_{jk}^{(4)}$ can be evaluated in a similar way. There are eight pathways (plus their complex conjugates) which contribute to $T_{21}^{(4)}$ or $T_{32}^{(4)}$. In terms of these correlation functions, the frequency dependent rate constants $K_{jk}(s)$ (to fourth order in V_{jk}) assume the form

$$K_{21}(s) = 2V_{12}^2\,\mathrm{Re}\langle G_{12}(s)\rho_1\rangle - V_{12}^4[\langle G_{12}(s)G_{22}(s)G_{12}(s)\rho_1\rangle_p + \langle G_{12}(s)G_{11}(s)G_{12}(s)\rho_1\rangle_p] - V_{12}^2V_{23}^2[\langle G_{23}(s)G_{22}(s)G_{12}(s)\rho_1\rangle_p + \langle G_{23}(s)G_{13}(s)G_{12}(s)\rho_1\rangle_c + \langle G_{12}(s)G_{13}(s)G_{12}(s)\rho_1\rangle_c] , \tag{3.10a}$$

$$K_{32}(s) = 2V_{23}^2\,\mathrm{Re}\langle G_{23}(s)\rho_2\rangle - V_{23}^4[\langle G_{23}(s)G_{22}(s)G_{23}(s)\rho_2\rangle_p + \langle G_{23}(s)G_{33}(s)G_{23}(s)\rho_2\rangle_p] - V_{12}^2V_{23}^2[\langle G_{23}(s)G_{22}(s)G_{12}(s)\rho_2\rangle_p + \langle G_{23}(s)G_{13}(s)G_{12}(s)\rho_2\rangle_c + \langle G_{23}(s)G_{13}(s)G_{23}(s)\rho_2\rangle_c] , \tag{3.10b}$$

$$K_{31}(s) = V_{12}^2V_{23}^2[\langle G_{23}(s)G_{13}(s)G_{12}(s)\rho_1\rangle_c + \langle G_{23}(s)G_{22}(s)G_{12}(s)\rho_1\rangle_p] . \tag{3.10c}$$

The other three rate constants, $K_{12}(s)$, $K_{23}(s)$, and $K_{13}(s)$, may be obtained from Eqs. (3.10) by interchanging the indexes 1 and 3 in $K_{32}(s)$, $K_{21}(s)$, and $K_{31}(s)$, respectively. The diagonal elements of the rate matrix are given by

$$K_{jj}(s) = -\sum_{k\neq j} K_{kj}(s) . \tag{3.11}$$

Equations (3.11) guarantee the conservation of probability. So far, we have expressed all the matrix elements of $K_{jk}(s)$ to fourth order in the nonadiabatic coupling in terms of the quantities $\langle G_{jk}(s)\rho_r\rangle$, $\langle G_{j'}(s)G_{kh}(s)G_{nm}(s)\rho_r\rangle_c$ and $\langle G_{j'}(s)G_{kk}(s)G_{nm}(s)\rho_r\rangle_p$. In the coming sections we shall calculate these quantities using a specific model for solvation.

IV. SLOW SOLVENT FLUCTUATIONS: THE STATIC APPROXIMATION

The nuclear Hamiltonian $H_j(Q)$ may be partitioned into the following terms:

$$H_j(Q) = E_j + H_B + U_j , \tag{4.1}$$

where E_j represents the electronic energy of the state $|j\rangle$ and H_B represents the Hamiltonian of the bath, which is taken to be a polar medium. U_j denotes the interaction between the electron system and the medium. In electron transfer processes in a polar medium it is common to adopt the following electrostatic model for U_j[9,10,22,23]:

$$U_j = -\int d\mathbf{r}\,\mathbf{D}_j(\mathbf{r})\cdot\mathbf{P}(\mathbf{r}) . \tag{4.2}$$

Downloaded 21 Jun 2002 to 128.151.176.185. Redistribution subject to AIP license or copyright, see http://ojps.aip.org/jcpo/jcpcr.jsp

Here $\mathbf{D}_j(\mathbf{r})$ is the electrostatic field produced by the charge distribution of the system in the $|j\rangle$ state, and $\mathbf{P}(\mathbf{r})$ is the polarization of the solvent at point $\mathbf{r}$. It should be emphasized that U_j depends on a macroscopic number of polarization degrees of freedom $\mathbf{P}(\mathbf{r})$, which undergo complicated motions resulting from thermal fluctuations. The statistical properties of U_j contain all the relevant information for our problem. We shall model U_j as Gaussian random variables. This is a common assumption in electron transfer theories.[8–10,12] It has been recently verified by an extensive numerical simulation of outer sphere electron transfer in water.[24]

In this section we shall evaluate the rate constant in the static limit, which generally holds for ET processes. This limit is introduced as follows. Coherences in condensed phases are usually subject to fast *dephasing* processes resulting from the solvent motions.[16] Consequently, the coherence Green functions [$\hat{G}_{jk}(t)$ with $j\neq k$] are expected to decay rapidly, on the dephasing timescale. The latter is typically in the picosecond to femtosecond range, as can be seen from the linewidths of optical transitions in solution. Pure dephasing processes do not affect the diagonal elements of the density matrix (populations) so that the typical time scales of $\hat{G}_{kk}(t)$ are of the order of the lifetime of the electronic states, which may be much larger (typically in the nanosecond range). The static approximation is based on this observation and assumes that the solvent motions are slow compared with the fast dephasing time (but not necessarily compared with the timescale of change of populations).[17] We therefore neglect all solvent motions in the coherence Green functions but include solvent relaxation in the population Green functions. This situation is common in spectral line broadening in condensed phases and is known as spectral diffusion. When the static (Classical Condon) approximation is made, we replace the coherence Green functions by[25]

$$G_{nm}(t)\cong\exp(-iH_{nm}t)=\exp(-iE_{nm}t-iU_{nm}t)\,,\qquad n\neq m \tag{4.3}$$

with

$$\begin{aligned}H_{nm}&\equiv H_n-H_m\,,\\ E_{nm}&\equiv E_n-E_m\,,\\ U_{nm}&\equiv U_n-U_m\,.\end{aligned} \tag{4.4}$$

In the static limit, the correlation functions appearing in Eqs. (3.10) assume the form

$$\langle G_{nm}(s)\rho_r\rangle=\int_0^\infty dt\exp(-st-iE_{nm}t)\times\langle\exp(-iU_{nm}t)\rho_r\rangle \tag{4.5a}$$

$$\begin{aligned}&\langle G_{j'}(s)G_{kk}(s)G_{nm}(s)\rho_r\rangle_p\\ &\quad=(2\pi)^2\int_0^\infty dt\exp(-st)\int dx\,dy\,\frac{s/\pi}{s^2+x^2}\,\frac{s/\pi}{s^2+y^2}\\ &\quad\times\langle\delta(x-H_{j'})[\hat{G}_{kk}(t)-\hat{G}_{kk}(\infty)]\\ &\quad\times\delta(y-H_{nm})\rho_r\rangle\,,\end{aligned} \tag{4.5b}$$

$$\begin{aligned}&\langle G_{j'}(s)G_{kh}(s)G_{nm}(s)\rho_r\rangle_c\\ &\quad=2\,\mathrm{Re}\int_0^\infty dt_3\int_0^\infty dt_2\int_0^\infty dt_1\exp[-(s+iE_{j'})t_3\\ &\qquad-(s+iE_{kh})t_2-(s+iE_{nm})t_1]\\ &\quad\times\langle\exp(-iU_{j'}t_3-iU_{kh}t_2-iU_{nm}t_1)\rho_r\rangle\,.\end{aligned} \tag{4.5c}$$

Equations (4.5) may be evaluated for the Gaussian model by using the cumulant expansion to second order in the interactions U_j, and then performing the time integrations. The first correlation function [Eq. (4.5a)] appears in nonadiabatic ET theories and was calculated previously.[12] In Appendix A we calculate Eq. (4.5a) and the s-dependent population correlation function [Eq. (4.5b)], and in Appendices B and C we calculate the corresponding coherence correlation function [Eq. (4.5c)]. When these expressions are substituted in Eq. (3.10) we obtain the full frequency dependent rate of the generalized rate equation. For the sake of clarity we shall concentrate now on the $s=0$ limit of the rate constant, $K_{jk}(0)\equiv K_{jk}$. This is the rate appearing in the ordinary rate Eqs. (2.17). Our rate expression is given in terms of several physical quantities. We first define the free energy change for the $|j\rangle$ to $|n\rangle$ transition

$$\Delta G^0_{jn}\equiv\langle H_j\rho_j\rangle-\langle H_n\rho_n\rangle \tag{4.6}$$

and the vertical transition energy for this transition when the system is in state $|m\rangle$

$$\Delta E^m_{jn}\equiv\langle(H_j-H_n)\rho_m\rangle\,. \tag{4.7}$$

Note that $\Delta E^m_{jn}=-\Delta E^m_{nj}$ and $\Delta G^0_{jn}=-\Delta G^0_{nj}$.

We next introduce the solvent Marcus reorganization energy for the $|j\rangle$ to $|k\rangle$ transition[9]

$$\lambda_{jk}\equiv\frac{\langle U^2_{jk}\rho_B\rangle}{2k_BT}\equiv\frac{\Delta^2_{jk}}{2k_BT}\,, \tag{4.8}$$

where ρ_B is given by Eq. (2.9) with H_j replaced by H_B. The reorganization energy parameter in the $|j\rangle$ state is

$$\lambda_j\equiv\frac{\langle U_{jk}U_{jm}\rho_B\rangle}{2k_BT} \tag{4.9}$$

where j, k, and m are the permutations of 1, 2, and 3. It can easily be shown that

$$\lambda_{jk}=\lambda_j+\lambda_k\,,\quad j\neq k.$$

In the high-temperature limit we further have (see Appendix D)

$$\begin{aligned}\Delta E^n_{nm}&=\Delta G^0_{nm}-\lambda_{nm}\,,\\ \Delta E^m_{nm}&=\Delta G^0_{nm}+\lambda_{nm}\,,\\ \Delta E^k_{nm}&=\Delta G^0_{nm}+\lambda_n-\lambda_m\,,\quad k\neq n,m.\end{aligned} \tag{4.10}$$

In Fig. 2 we display the energetic parameters introduced here. We also define the following combinations of parameters:

$$\eta^r_{jk}=\sqrt{R_{jk}}\,\frac{\Delta E^r_{jm}\lambda_k+\Delta E^r_{km}\lambda_j}{\lambda_{jk}}\,, \tag{4.11a}$$

where j, k, and m are the permutations of 1, 2, and 3 and

$$R_{jk}=\frac{\lambda_{jk}}{[\lambda_{12}\lambda_{23}-\lambda^2_2]2k_BT}\,. \tag{4.11b}$$

Downloaded 21 Jun 2002 to 128.151.176.185. Redistribution subject to AIP license or copyright, see http://ojps.aip.org/jcpo/jcpcr.jsp

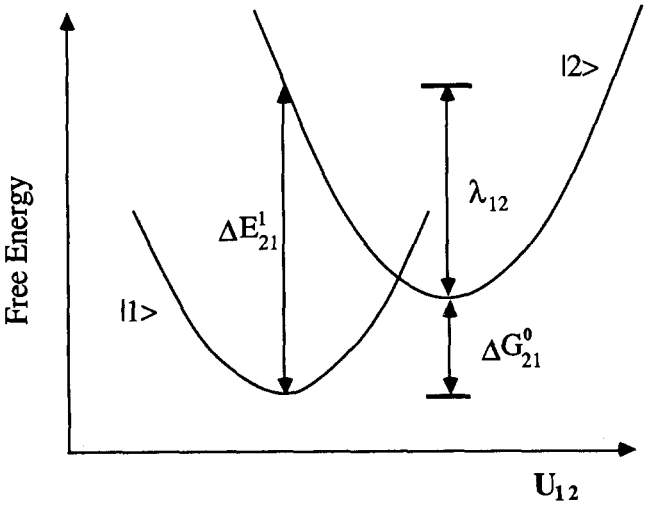

FIG. 2. Configuration coordinate scheme showing the transition free energy ΔG^0_{21} the reorganization energy λ_{12} and the vertical transition energy ΔE^1_{21}. Similar schemes apply for the other pairs of levels (1 and 3, 2 and 3).

R_{jk} depends strongly on the correlations of the various U_j. A measure of these correlations is given by the correlation coefficient γ

$$\gamma \equiv \frac{\langle U_{jk} U_{km} \rho_B \rangle}{\Delta_{jk} \Delta_{km}}, \tag{4.11c}$$

where j, k, and m are permutations of 1, 2, and 3. The Schwartz inequality implies that $|\gamma| \leqslant 1$. If the various U_j are totally uncorrelated and have equal fluctuations, i.e., $\langle U_j U_k \rho_B \rangle = \langle U^2 \rho_B \rangle \delta_{jk}$ then $\gamma = -1/2$. If on the other hand, they are fully correlated, i.e., $\langle U_j U_k \rangle = \pm \langle U^2 \rangle$ we get $\gamma = \pm 1$. The latter case, in which R_{jk} diverges is discussed in Appendix E. Making use of the correlation functions evaluated in Appendices A and B, and performing a Pade resummation of the series (3.2), similar to what was done in Ref. 12 for the two-site problem, we obtain our final expression for the rate matrix in the static limit:

$$K_{21} = \frac{\sigma_{21}}{1 + \sigma_{12}\tau_a + \sigma_{21}\tau_b + \sigma_{32}\tau_c} + \frac{2\pi}{\hbar} V_{12}^2 V_{23}^2 \times [R_{12} I(\eta^1_{12}) S_{12}(\Delta E^1_{12}) + R_{23} I(\eta^1_{23}) S_{23}(\Delta E^1_{23})], \tag{4.12a}$$

$$K_{32} = \frac{\sigma_{32}}{1 + \sigma_{32}\tau'_a + \sigma_{23}\tau'_b + \sigma_{12}\tau_c} + \frac{2\pi}{\hbar} V_{12}^2 V_{23}^2 \times [R_{12} I(\eta^2_{12}) S_{12}(\Delta E^2_{12}) + R_{23} I(\eta^2_{23}) S_{23}(\Delta E^2_{23})], \tag{4.12b}$$

$$K_{31} = \sigma_{21}\sigma_{32}\tau_c + \frac{2\pi}{\hbar} V_{12}^2 V_{23}^2 [R_{13} I(\eta^1_{13}) S_{13}(\Delta E^1_{13}) - R_{12} I(\eta^1_{12}) S_{12}(\Delta E^1_{12}) - R_{23} I(\eta^1_{23}) S_{23}(\Delta E^1_{23})]. \tag{4.12c}$$

Each rate constant has two terms. The first is coming from the population pathways and the second from the coherence pathways. The population term depends on σ_{jn} and various solvent timescales τ_j, τ'_j. σ_{jn} is the nonadiabatic transition rate from state n to j,

$$\sigma_{jn} \equiv (2\pi/\hbar) V^2_{jn} S_{jn}(\Delta E^n_{jn}). \tag{4.13}$$

and S_{jn} is the Franck–Condon weighted density of states

$$S_{jn}(x) = \frac{1}{\sqrt{4\pi k_B T \lambda_{jn}}} \exp\left[- \frac{x^2}{4 k_B T \lambda_{jn}} \right]. \tag{4.14}$$

τ_a, τ_b, τ'_a, τ'_b and τ_c are characteristic solvation time scales, defined as follows. We first introduce two time scale functions

$$\tau_{jk}(q) = \int_0^\infty dt \left\{ \frac{1}{\sqrt{1 - M^2_{jk}(t)}} \exp\left[\frac{2 M_{jk}(t) q^2}{1 + M_{jk}(t)} \right] - 1 \right\}, \tag{4.15}$$

$$\tau(q,q') = \int_0^\infty dt \left\{ \frac{1}{\sqrt{1 - M^2(t)}} \times \exp\left[\frac{2qq' M(t) - (q^2 + q'^2) M^2(t)}{1 - M^2(t)} \right] - 1 \right\}. \tag{4.16}$$

Here q and q' are dimensionless parameters. $M_{jk}(t)$ and $M(t)$ are the solvent correlation functions

$$M_{jk}(t) = \frac{\langle \exp(iH_B t) U_{jk} \exp(-iH_B t) U_{jk} \rho_B \rangle}{\Delta^2_{jk}}, \tag{4.17a}$$

$$M(t) = \frac{\langle \exp(iH_B t) U_{23} \exp(-iH_B t) U_{21} \rho_B \rangle}{\Delta_{23}\Delta_{12}}. \tag{4.17b}$$

We further define

$$q_{nm} \equiv \frac{\Delta E^m_{nm}}{\sqrt{4 k_B T \lambda_{nm}}}. \tag{4.18}$$

In terms of these quantities we have $\tau_a = \tau_{12}(q_{12})$, $\tau_b = \tau_{12}(q_{21})$, $\tau'_a = \tau_{23}(q_{32})$, $\tau'_b = \tau_{23}(q_{23})$, $\tau_c = \tau(q_{32}, q_{12})$. Note that $q_{nm} \neq q_{mn}$ and that τ'_a and τ'_b are obtained from τ_a and τ_b, respectively, by interchanging the indexes 1 and 3. $\tau_{jk}(q)$ was calculated and analyzed previously in detail.[12] $\tau_{jk}(q) = \tau(q,q)$ provided we set $M_{jk}(t) = M(t)$. We further note that M_{jk} is normalized such that $M_{jk}(0) = 1$. $M(0)$, however, depends on the correlations among the various U_j and $M(0) = -\gamma$ where γ is the correlation coefficient introduced in Eq. (4.11c). In a polar medium, U_{jn} are related to the solvent polarization [Eq. (4.2)]. $M_{jk}(t)$ and $M(t)$ can then be expressed in terms of the two point correlation function of the polarizaton, which in turn is related to the solvent frequency and wave vector dependent dielectric function $\epsilon(k,\omega)$. In the dielectric continuum model we neglect the k dependence of ϵ and relate these correlation functions to $\epsilon(\omega) \equiv \epsilon(k = 0, \omega)$. These expressions were given elsewhere[12] and will not be repeated here. We have calculated the time scale function $\tau(q,q')$ assuming that the solvation coordinates of the various states are totally uncorrelated and have the same fluctuations, i.e.,

$$\langle U_j U_k \rho_B \rangle = \langle U^2 \rho_B \rangle \delta_{jk}. \tag{4.19}$$

In this case we have from Eq. (4.17b) $M(0) = 0.5$. We further assumed that $M(t)$ decays exponentially with time

Downloaded 21 Jun 2002 to 128.151.176.185. Redistribution subject to AIP license or copyright, see http://ojps.aip.org/jcpo/jcpcr.jsp

as predicted by the Debye model of dielectric fluctuations.[17] We thus set $M(t) = 0.5\exp(-t/\tau_0)$. The time scale function $\tau(q,q')$ for this model is displayed in Fig. 3. The function $I(x)$ is given by

$$I(x) = -\int_0^\infty t\cos(xt)\exp(-t^2/2)\,dt. \tag{4.20}$$

We have constructed the following approximation for $I(x)$,

$$I(x) \cong \begin{cases} \dfrac{-1+0.5851x^2}{1+0.4149x^2+0.1235x^4}, & |x|<2.1 \\ \dfrac{-1+0.5994x^2}{11.2551-3.8396x^2+0.5994x^4}, & |x|\geqslant 2.1 \end{cases}. \tag{4.21}$$

The asymptotic behavior of $I(x)$ is

$$I(x) = \begin{cases} 1/x^2, & x \gg 1 \\ -1+x^2, & x \ll 1 \end{cases}. \tag{4.22}$$

$I(x)$ is displayed in Fig. 4. The dashed line in Fig. 4 shows the difference between the exact [Eq. (4.20)] and the approximation [Eq. (4.21)] for $I(x)$. As noted in Sec. III, K_{12}, K_{23}, and K_{13} can be obtained from K_{32}, K_{21}, and K_{31}, respectively, by interchanging the indexes 1 and 3. The diagonal elements K_{11}, K_{22}, and K_{33} are given by Eq. (3.11). Equations (4.12) thus provide the entire rate matrix for the system.

V. SEQUENTIAL AND SUPEREXCHANGE ELECTRON TRANSFER

We shall now analyze our rate matrix [Eqs. (4.12)]. We first note that to second order in V_{jk}, Eqs. (4.12) reduce to the well-known nonadiabatic rates[9] $K_{21} = \sigma_{21}$, $K_{32} = \sigma_{32}$, $K_{31} = 0$. When setting $V_{23} = 0$ all rates vanish except for K_{12} and K_{21},

$$K_{21} = \frac{\sigma_{21}}{1+\sigma_{12}\tau_a+\sigma_{21}\tau_b}, \tag{5.1a}$$

$$K_{12} = \frac{\sigma_{12}}{1+\sigma_{12}\tau_a+\sigma_{21}\tau_b}. \tag{5.1b}$$

Equations (5.1) have been derived and analyzed previously.[12] τ_a and τ_b are typical solvent timescales. Equations (5.1) interpolate from the nonadiabatic limit ($\tau_a,\tau_b \to 0$) to the adiabatic limit, where τ_a and τ_b are long and the rate becomes equal to an inverse solvent time scale. The first term in K_{21}, K_{32}, and K_{31} [Eqs. (4.12a)–(4.12c)] is an extension of Eqs. (5.1) to a three-site system. It depends on five different solvent time scales τ_a, τ_b, τ_c, τ_a', τ_b'. Like Eqs. (5.1), the first term interpolates between the nonadiabatic rate (for $\tau_j \to 0$) to an inverse average time scale (as $\tau_j \to \infty$). The second term in K_{21} and K_{32} comes from a coherent process in which the electron transfers between the states via coherences without passing through a population. K_{31} [Eq. (4.12c)] has two terms. The first represents the process in which the electron does pass through the population of the state $|2\rangle$, but before it equilibriates with the solvent at the state $|2\rangle$, the electron transfers to state $|3\rangle$. This term is represented by diagrams (i) and (ii) in Fig. 1(b). The second term in Eq. (4.12c) represents the process in which the electron tunnels from state $|1\rangle$ to state $|3\rangle$ without actually passing through the state $|2\rangle$. This term is represented by diagram (iii) in Fig. 1(b).

We shall now consider K_{31} more closely. For simplicity we assume that the relaxation of the system is sufficiently rapid, $\tau_c \to 0$, so that the only quantity we need to consider in K_{31} is the second term in Eq. (4.12c). We shall examine a few limiting cases of Eq. (4.12c). We first consider the case whereby the energy level $|2\rangle$ is sufficiently far from the energy levels $|1\rangle$ and $|3\rangle$, i.e.,

$$\Delta E_{21}^{\ddagger} \gg \sqrt{\lambda_{12}k_BT}\,, \quad \Delta E_{23}^{\ddagger} \gg \sqrt{\lambda_{23}k_BT}\,. \tag{5.2}$$

Equation (5.2) implies that the activation energies $\Delta G_{12}^{*} \equiv (\Delta G_{12}^{0}-\lambda_{12})^2/4\lambda_{12}$ and $\Delta G_{23}^{*} \equiv (\Delta G_{23}^{0}+\lambda_2-\lambda_3)^2/4\lambda_{23}$ are much larger than k_BT. This limit is where the conventional superexchange theory is usually formulated.[7,26,27] In this case, by using the asymptotic expression Eq. (4.22) of $I(x)$, Eq. (4.12c) assumes the form

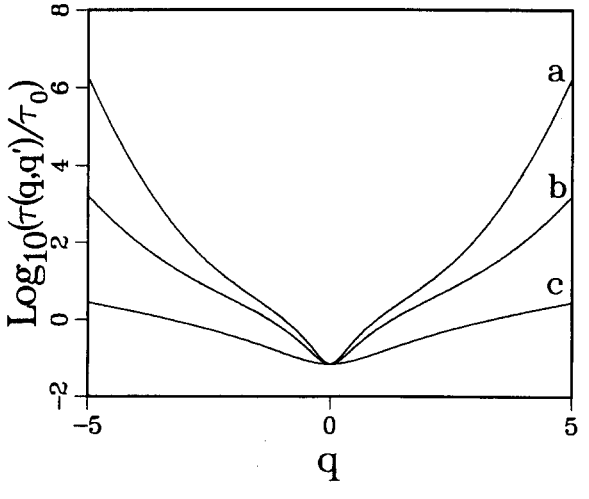

FIG. 3. Solvent timescale function $\tau(q,q')$ [Eq. (4.16)]. Curves a, b, and c correspond to $q' = q$, $q' = 0.6q$ and $q' = 0.2q$, respectively. We also assume $M(t) = 0.5\exp(t/\tau_0)$ (see the text).

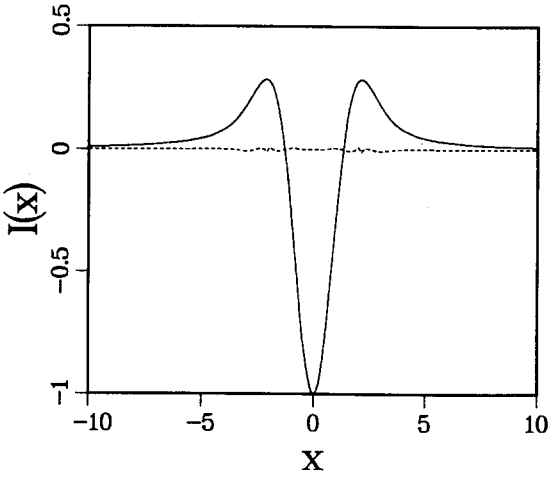

FIG. 4. Auxiliary function $I(x)$ [Eq. (4.20)] (solid line). The dashed line represents the difference between the exact curve [Eq. (4.20)] and the approximation [Eq. (4.21)].

Downloaded 21 Jun 2002 to 128.151.176.185. Redistribution subject to AIP license or copyright, see http://ojps.aip.org/jcpo/jcpcr.jsp

$$K_{31} = (2\pi/\hbar)|V_{SE}|^2 S_{13}(\Delta E^1_{13}) \tag{5.3a}$$

with

$$V_{SE} = \frac{V_{12}V_{23}}{\Delta E^1_{12}(\lambda_3/\lambda_{13}) + \Delta E^1_{32}(\lambda_1/\lambda_{13})} . \tag{5.3b}$$

Equations (5.3) may be obtained using the Fermi Golden rule and the superexchange coupling matrix element V_{SE}. Note that in this limit the rate satisfies the detailed balance condition

$$K_{31}/K_{13} = \exp(-\Delta G^0_{31}/k_B T) . \tag{5.4}$$

We next consider another limiting case where all the three states are completely degenerate, i.e., $\Delta E^1_{12} = \Delta E^1_{23} = \Delta E^1_{13} = 0$. We further assume $\lambda_1 = \lambda_2 = \lambda_3 \equiv \lambda$. We then obtain from Eq. (4.12c)

$$K_{31} = \frac{2\pi}{\hbar}|V_{SE}|^2 S_{13}(0) , \tag{5.5a}$$

where the superexchange coupling matrix element is

$$V_{SE} = \frac{V_{12}V_{23}}{\sqrt{3\lambda k_B T}} . \tag{5.5b}$$

Equations (5.5) may be rationalized using a simple physical argument. The variance of the energy level fluctuations is $\sim\sqrt{\lambda k_B T}$. V_{SE} is thus given by $V_{12}V_{23}$ divided by a typical thermal energy fluctuation.

The primary electron transfer process in the photosynthetic reaction center (RC)[4] involves a transition from a photoexcited bacteriochlorophyll dimer (P) to bacteriopheophytin (H). In this process the electron transfers over a distance of 17 Å in 2.8 ps. Since a direct (through space) coupling between P and H is excluded by their large separation, it has been suggested that the bacteriochlorophyll monomer (B), which is located between P and H plays an active role in this event. This system may thus be described by the present three site-model with states $|1\rangle$, $|2\rangle$, and $|3\rangle$ corresponding to the electron on P, B, and H, respectively. A controversial issue[26–28] is the relative magnitude of the superexchange and the sequential mechanisms in this system. In the calculations presented in the following figures we have used some characteristic parameters of the reaction center ET system. We have calculated K_{31} using Eq. (4.12c) and the results are displayed in Fig. 5 as a function of $\Delta E^1_{21} = \Delta G^0_{21} + \lambda_{12}$ for different values of ΔE^1_{13}. The dashed line in Fig. 5 represents the conventional superexchange rate expression [Eqs. (5.3)] which breaks down when level 2 is not well separated from levels 1 and 3. Recent ultrafast measurements performed on the reaction center[29] have probed the appearance of the state $|3\rangle$, following the optical preparation of state $|1\rangle$. Since the appearance of $|3\rangle$ may not be necessarily a single exponential, it is useful to introduce a single characteristic timescale $\bar{\tau}$ which is analogous to the mean first passage time, defined as follows:

$$\bar{\tau} = \int_0^\infty [p_3(\infty) - p_3(t)]\, dt . \tag{5.6}$$

Here $p_3(t)$ is the solution of the generalized master equation with the initial condition $p_2(0) = p_3(0) = 0, p_1(0) = 1$. Using the definition of $\bar{\tau}$ and the general relation of Laplace transforms $p_3(\infty) = \lim_{s\to 0} s p_3(s)$ we obtain

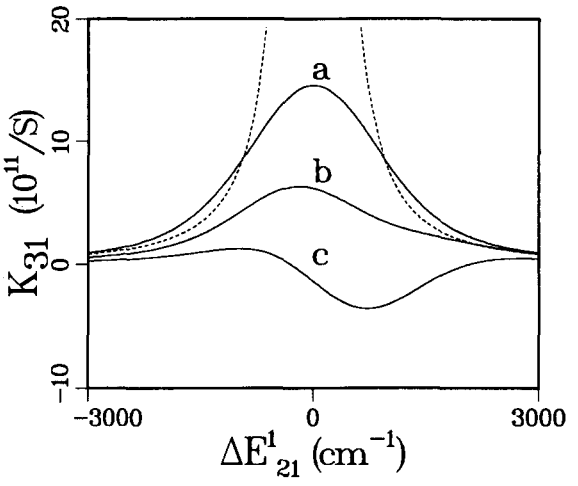

FIG. 5. Dependence of the superexchange rate K_{31} on ΔE^1_{21}. Curves a, b, and c correspond to $\Delta E^1_{13} = 0$, 700 and 1200 cm^{-1}, respectively. The other parameters in this calculation are: $\lambda_{12} = 1000\ cm^{-1}$, $\lambda_{23} = 1500\ cm^{-1}$, $\lambda_{13} = 2000\ cm^{-1}$, $V_{12} = 80\ cm^{-1}$, $V_{23} = 6V_{12}$, $T = 300$ K. The dashed line represents the conventional superexchange rate [Eqs. (5.3)] with $\Delta E^1_{13} = 0$.

$$\bar{\tau} = -\frac{X(K_{11} + K_{22} + K_{33}) + K_{31}Y}{Y^2} \tag{5.7}$$

with

$$X = K_{21}K_{32} - K_{31}K_{22} , \tag{5.8a}$$

$$Y = (K_{21} - K_{22})(K_{31} - K_{33}) - (K_{23} - K_{21})(K_{32} - K_{31}) , \tag{5.8b}$$

$$K_{jk} \equiv K_{jk}(0) . \tag{5.8c}$$

An important feature of $\bar{\tau}$ is that it only depends on the rate matrix $K_{jk}(s)$ at $s = 0$. Even though the dynamics may require the full frequency dependent rate $K_{jk}(s)$, $\bar{\tau}$ depends only on $K_{jk}(0)$. Ignoring the reverse rates K_{13}, K_{12}, and K_{23} and assuming $K_{32} \gg K_{21}$ which is the situation for the reaction center, Eq. (5.7) reduces to

$$\bar{\tau} = \frac{1}{K_{31} + K_{21}} . \tag{5.9}$$

We shall now introduce the following ratio as a measure of the relative contribution of the superexchange mechanism to the total rate:

$$R \equiv \frac{K_{31}}{K_{31} + K_{21}} . \tag{5.10}$$

When $R \ll 1$ the sequential transfer dominates, and for $R \to 1$ the superexchange transfer dominates. Figures 6–8 display the dependence of R on the energy ΔE^1_{21} for different values of ΔE^1_{13}, coupling V_{12}, and reorganization energy λ_{12}. In all figures $R \to 1$ for large values of ΔE_{21}, indicating that the rate becomes dominated by superexchange. The way in which R attains its limiting value depends on the other parameters, as shown in Figs. 6–8.

Our rate expression [Eqs. (4.12)] was obtained in the high temperature limit. It may be extended to low tempera-

Downloaded 21 Jun 2002 to 128.151.176.185. Redistribution subject to AIP license or copyright, see http://ojps.aip.org/jcpo/jcpcr.jsp

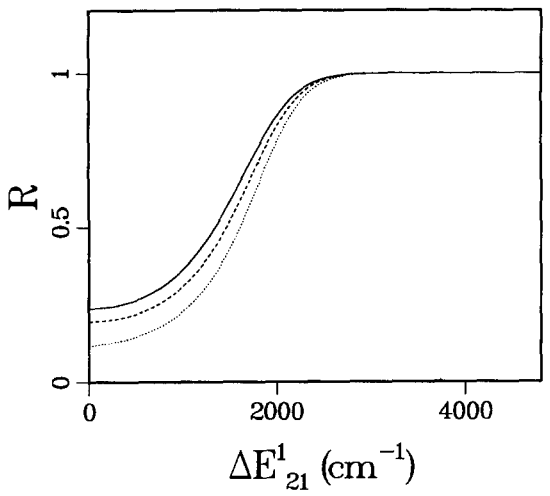

FIG. 6. Relative contribution of the superexchange mechanism R [Eq. (5.10)] is displayed vs ΔE^1_{21}. The solid, dashed, the dotted lines correspond to $\Delta E^1_{13} = 0$, 400 and 700 cm^{-1}, respectively. The other parameters are: $\lambda_{13} = 2000$ cm^{-1}, $\lambda_{23} = 1500$ cm^{-1}, $\lambda_{12} = 1000$ cm^{-1}, $V_{12} = 80$ cm^{-1}, $V_{23} = 6\,V_{12}$, $T = 300$ K.

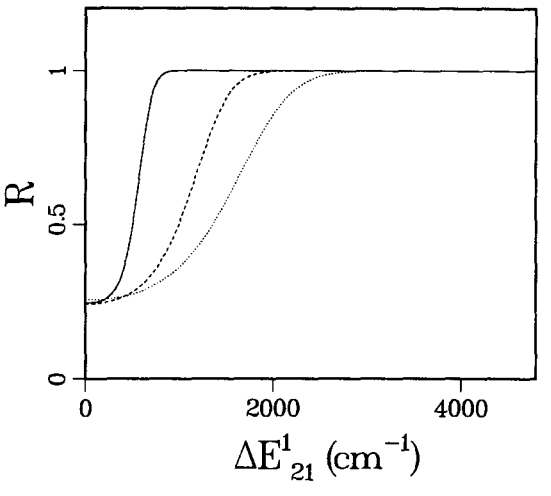

FIG. 8. Relative contribution of the superexchange mechanism R [Eq. (5.10)] is displayed vs ΔE^1_{21} for different values of the reorganization energy λ_{12}. The solid, dashed, and dotted lines correspond to $\lambda_{12} = 100$, 500 and 1000 cm^{-1}, respectively. The other parameters are $\Delta E^1_{13} = 0$, $\lambda_{13} = 2000$ cm^{-1}, $\lambda_{23} = 2000$ cm^{-1}, $V_{12} = 80$ cm^{-1}, $V_{23} = 6\,V_{12}$, $T = 300$ K.

tures by adopting a more specific model for H_B and U_j. A common model in electron transfer theories assumes that U_j is dominated by a single harmonic coordinate representing an intramolecular or intermolecular vibration with frequency ω. In this case Eqs. (4.12) should be modified by replacing all $k_B T$ factors by the average oscillator energy $\langle\epsilon\rangle$[9]

$$\langle\epsilon\rangle = \frac{\hbar\omega}{2}\coth\left(\frac{\hbar\omega}{2k_B T}\right). \tag{5.11}$$

In the high-temperature ($k_B T \gg \hbar\omega$) limit $\langle\epsilon\rangle = k_B T$. When $k_B T$ in Eqs. (4.12) is replaced by $\langle\epsilon\rangle$ [Eq. (5.11)] we obtain a rate expression which is not restricted to the high temperature limit. We have used the present theory[30] for K_{31} together with Eq. (5.11) to analyze the temperature dependence of the ET rate observed in Rhodopseudomonas viridis.[29]

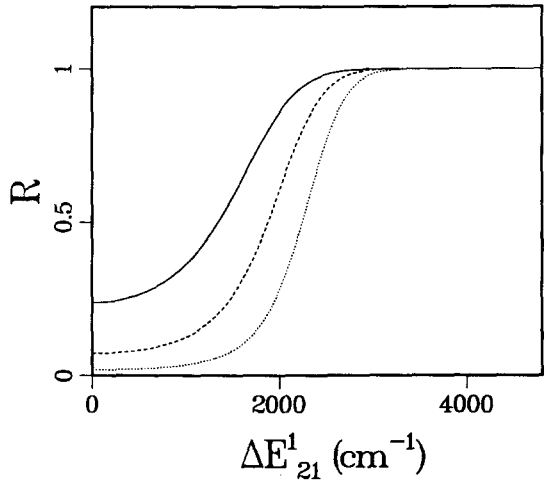

FIG. 7. Relative contribution of the superexchange mechanism R [Eq. (5.10)] is displayed vs ΔE^1_{21}. $V_{12} = 80\,cm^{-1}$ (solid line), $40\,cm^{-1}$ (dashed line) and $20\,cm^{-1}$ (dotted line). Other parameters are: $\lambda_{13} = 2000$ cm^{-1}, $\lambda_{23} = 1500$ cm^{-1}, $\lambda_{12} = 1000$ cm^{-1}, $\Delta E^1_{13} = 0$, $V_{23} = 6\,V_{12}$, $T = 300$ K.

It should be noted that for certain values of the parameters, K_{31} [Eqs. (4.12c)] and $\tau(q,q')$ can become negative. This may happen when $\Delta E_{13} \gg \sqrt{k_B T \lambda_{13}}$ and level E_2 is located between E_1 and E_3 (curve c in Fig. 5). In this case the system cannot be described by simple rate equations and one should calculate the complete frequency dependent rate $K_{jk}(s)$ which enters in the generalized rate equation [Eq. (2.12)]. In the next section we present the exact solution for the rate (to infinite order in the nonadiabatic coupling) in the limit of fast solvent fluctuations. There, too, $K_{31}(0)$ may become negative for the same reasons.

VI. FAST SOLVENT FLUCTUATIONS: HOMOGENEOUS DEPHASING

In typical electron transfer systems in condensed phases, the solvent has a complex dynamics characterized by many different time scales. In the previous section we adopted the static limit which assumes that the solvent time scales are slow compared with the inverse characteristic line broadening (spectral width of S_{jn}). This limit is applicable in condensed phases where the linewidth is extremely broad. It should be noted, however, that assuming a Gaussian statistics for the solvation coordinate, it is possible to solve for the correlation functions exactly for an arbitrary solvent time scale, i.e., without invoking the static limit. In the theories of spectral lineshapes, it is common to use stochastic models which can be solved for an arbitrary solvent time scale.[16,31] The stochastic models are, however, classical and do not allow the solvent to be affected by the system. Consequently they show no Stokes shift. We have developed a more general exactly solvable model which does not suffer from these limitations.[32] The general solution is relatively simple in the time domain, but requires a triple Laplace transform similar to Eq. (4.5c) to get the correlation functions in the frequency domain. It is the performing of these triple integrations that makes the general solution more complicated. The results of

Downloaded 21 Jun 2002 to 128.151.176.185. Redistribution subject to AIP license or copyright, see http://ojps.aip.org/jcpo/jcpcr.jsp

the previous sections are the limit of that model when the solvent fluctuations are slow. It is instructive however to consider the reverse limit, i.e., when solvent fluctuations are fast compared with their inverse magnitude. In this limit the line shape is *homogeneously* broadened, in contrast with the static limit which corresponds to *inhomogeneous* broadening. The homogeneous dephasing model is less realistic for electron transfer. It is however exactly solvable to infinite order in the nonadiabatic coupling V. Its analysis thus provides a valuable insight on the limitations of our perturbative expansion [Eqs. (3.10)]. A serious limitation of the homogeneous model is that it is an infinite temperature limit in which $K_{jk} = K_{kj}$ so that at equilibrium all sites are equally populated. The model thus fails to predict the desired detailed balance condition at finite temperatures.

The equations of motion in the homogeneous dephasing model for an N-site system assume the form

$$\begin{aligned}\dot{\rho}_{jk} = &(-i)(E_j - E_k)\rho_{jk} - \Gamma_{jk}\rho_{jk} + iV_{k-1,k}\rho_{j,k-1} \\ &+ iV_{k,k+1}\rho_{jk+1} - iV_{j-1,j}\rho_{j-1,k} \\ &- iV_{j,j+1}\rho_{j+1,k} \end{aligned} \tag{6.1}$$

with

$$p_j(t) \equiv \langle j|\rho(t)|j\rangle , \tag{6.2a}$$

$$\rho_{jk}(t) \equiv \langle j|\rho(t)|k\rangle , \quad j \neq k . \tag{6.2b}$$

$p_j(t)$ represents the population on the site j and $\rho_{jk}(t)$ represents the coherence between the state j and state k. Γ_{jk} denotes the *pure dephasing* rate which satisfies the condition $\Gamma_{jj} = 0$. This condition implies that there is no damping for the populations. The exact rate constants for this model are

$$K_{21}(s) = K_{12}(s) = \mathrm{Re}\frac{2V_{12}^2 B_{13}(B_{23}B_{13} + V_{12}^2) - 2V_{12}^2 V_{23}^2 B_{13}}{\Delta} , \tag{6.3a}$$

$$K_{32}(s) = K_{23}(s) = \mathrm{Re}\frac{2V_{23}^2 B_{13}(B_{12}B_{13} + V_{23}^2) - 2V_{23}^2 V_{12}^2 B_{13}}{\Delta} , \tag{6.3b}$$

$$K_{31}(s) = K_{13}(s) = \mathrm{Re}\frac{2V_{12}^2 V_{23}^2 B_{13}}{\Delta} , \tag{6.3c}$$

where

$$B_{jk} = s + \Gamma_{jk} + i(E_j - E_k) , \tag{6.4}$$

$$\Delta = (B_{12}B_{13} + V_{23}^2)(B_{23}B_{13} + V_{12}^2) - V_{12}^2 V_{23}^2 . \tag{6.5}$$

We have calculated the rate constant $K_{31}(0)$ as function of the energy E_2 with different energies E_1 and E_3. The calculations displayed in Fig. 9 show that if $|E_1 - E_3| \ll \Gamma$, the rate $K_{31}(0)$ is always positive. However, if $E_1 - E_3 > \Gamma$ and E_2 is located between E_1 and E_3 the rate $K_{31}(0)$ then becomes negative. As E_2 is varied so that it is not between E_1 and E_3, the rate $K_{31}(0)$ becomes positive again. This is a similar situation to what we found for K_{31} in the previous section except that the dephasing rate Γ should be replaced by $\sqrt{4k_B T\lambda_{jk}}$. In this case one has to use the full frequency dependent rate, and the ordinary rate equation does not hold. Figure 10 displays the frequency dependence of $K_{31}(s)$, and shows that it vanishes as $s \to \infty$. It should be pointed out that the rate $K_{31}(s)$ always becomes positive for large s regardless of the other energy parameters. We next calculate the time-dependent population of state 3 when initially the electron is localized in state 1. We present two different calculations. First we solve the generalized master equation Eq. (2.12) exactly.

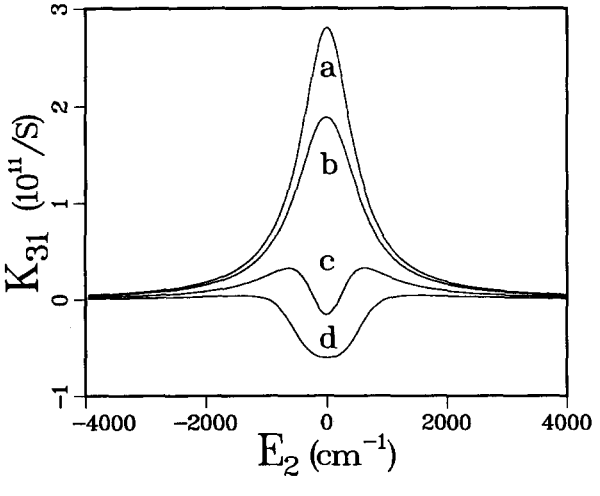

FIG. 9. Dependence of the exact superexchange rate K_{31} in the homogeneous dephasing model [Eq. (6.3c)] on energy E_2 for different values of energies E_1 and E_3. $E_3 = -E_1$. Curves a, b, c, and d correspond to $E_1 = 0$, 100, 250, and 500 cm^{-1}, respectively. The other parameters are $\Gamma = 500$ cm^{-1} $V_{12} = V_{23} = 100$ cm^{-1}. This figure shows that if $|E_1 - E_3|$ is large enough, the superexchange rate K_{31} may become negative for some values of E_2. This behavior is very similar to that in Fig. 5, where the superexchange rate K_{31} was obtained by using the static approximation.

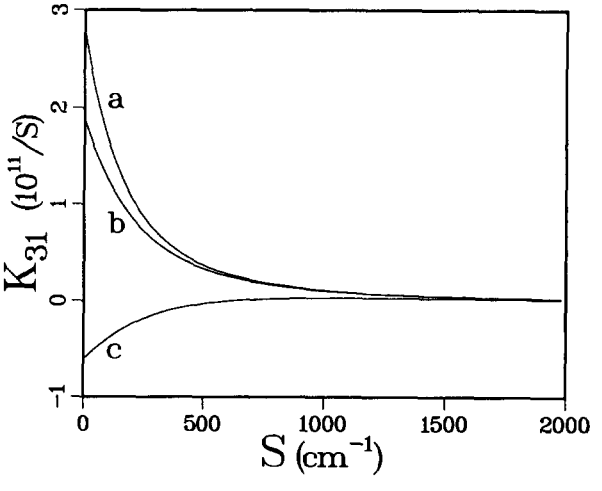

FIG. 10. Frequency-dependence of the superexchange rate $K_{31}(s)$ in the homogeneous dephasing model [Eq. (6.3c)]. $E_1 = -E_3$. Curves a, b, and c correspond to $E_1 = 0$, 100, and 500 cm^{-1}, respectively. The other parameters are: $\Gamma = 500$ cm^{-1} $V_{12} = V_{23} = 100$ cm^{-1}. Though it is not very clear in this figure, the rate $K_{31}(s)$ is always positive for large s [$K_{31}(s)$ becomes positive in curve c for $s > 600$ cm^{-1}].

Downloaded 21 Jun 2002 to 128.151.176.185. Redistribution subject to AIP license or copyright, see http://ojps.aip.org/jcpo/jcpcr.jsp

In the second calculation we approximate $K_{jk}(s)$ by $K_{jk}(0)$, and solve the ordinary rate equation Eq. (2.17). We have chosen parameters such that $K_{31}(0)$ is negative. The results are displayed in Figs. 11 and 12. The exact solutions of the generalized master equation are, of course, always positive. The solutions of the ordinary rate equation may yield a negative population for a short time but approach the exact solutions for long times. These calculations demonstrate that the negative value of $K_{31}(s)$ at $s=0$ is a signature of the breakdown of the ordinary rate equation at short times. As the dephasing rate Γ increases, the ordinary rate equation holds for shorter and shorter times (Fig. 12). When $\Gamma \to \infty$, the ordinary rate equations become exact.

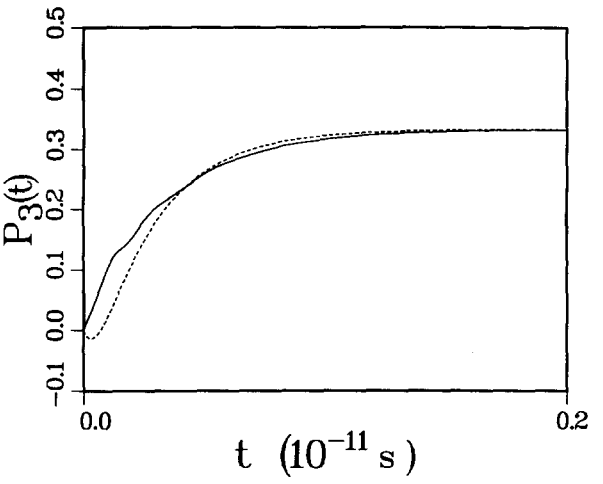

FIG. 12. Same as Fig. 11, but with a larger dephasing rate $\Gamma = 100\ \text{cm}^{-1}$. As the dephasing rate increases, the difference between the solution of the generalized rate equation (solid line) and the ordinary rate equation (dashed line) decreases.

VII. RELATION TO ULTRAFAST PUMP-PROBE SPECTROSCOPY

The model system studied in this article (electron transfer in a multisite system interacting with a thermal bath) is formally identical to the models commonly used in the studies of the nonlinear optical response and susceptibilities in condensed phases.[17(b)] In this section we elaborate on this analogy in detail. The density matrix formulation of optical (and nuclear magnetic resonance) line shapes is well developed[15] and by formulating rate theories in the same manner we gain a better insight on the relationship among these different observables. Multiphoton processes are naturally classified as coherent and incoherent, in complete analogy with the tunneling and the sequential pathways, respectively, appearing in the present rate theory. One well-known example is the classification of emission line shapes into Raman and fluorescence components. The Raman process is a direct event proceeding via coherences whereas fluorescence is a sequential process. At large detunings and in the absence of dephasing processes, the emission is purely of the Raman type. As the incident frequency is tuned on resonance, and when dephasing processes take place, the fluorescence becomes dominant.[16] This state of affairs is remarkably similar to the dominance of the sequential mechanism as the intermediate energy (E_2) is tuned closer to E_1 and E_3. In this section we shall focus on pump-probe spectroscopy[18–20] which bears the closest analogy with the rate theory developed in this article. Consider a three-level molecular system with energy levels E_g, E_e, and E_f (Fig. 13). At $t=0$ we subject the system to a short pump pulse with temporal envelope $\epsilon_1(t)$ and frequency ω_1. Subsequently, the system interacts with a second probe pulse $\epsilon_2(t-\tau)$ with frequency ω_2 centered around $t=\tau$, and the total absorption of the probe is recorded as a function of ω_1, ω_2 and τ. We further consider only resonant interactions (the rotating wave approximation) and assume that ω_1 is resonant with $E_e - E_g$ and ω_2 is resonant with $E_f - E_e$ (Fig. 13). Under these conditions we

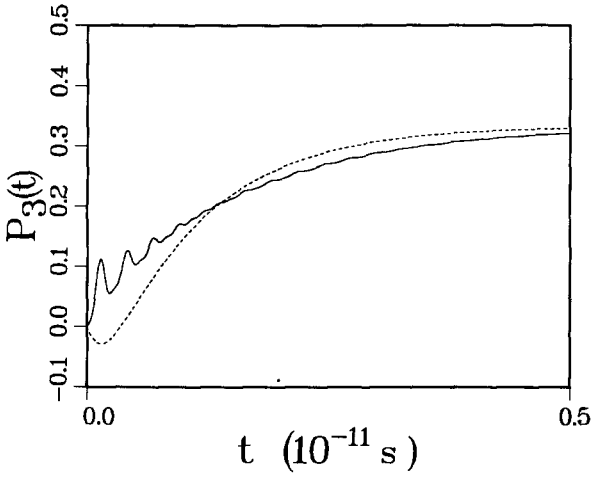

FIG. 11. Time dependence of the population $p_3(t)$ in the homogeneous dephasing model. The initial conditions are $p_1(0)=1$, $p_2(0)=p_3(0)=0$. The solid line represents the exact solution using the frequency dependent rate [Eqs. (6.3)] and the dashed line represents the solution of the ordinary rate equations with $\mathbf{K}(0)$. The parameters in this calculation are $E_1 = -E_3 = 100\ \text{cm}^{-1}$, $E_2 = 0\ \text{cm}^{-1}$, $V_{12} = V_{23} = 50\ \text{cm}^{-1}$ and $\Gamma = 20\ \text{cm}^{-1}$.

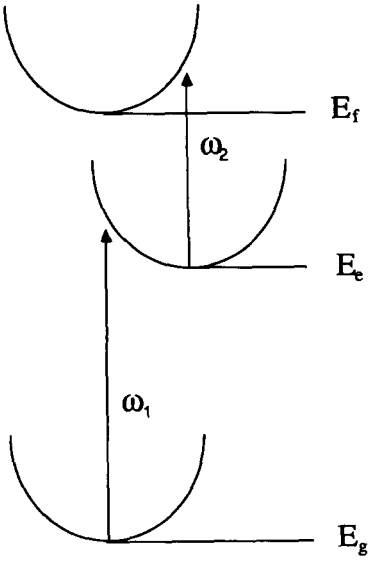

FIG. 13. Molecular level scheme for pump-probe spectroscopy. The pump field with frequency ω_1 is resonant with the $|g\rangle$ to $|e\rangle$ transition, whereas the probe (ω_2) is resonant with the $|e\rangle$ to $|f\rangle$ transition.

Downloaded 21 Jun 2002 to 128.151.176.185. Redistribution subject to AIP license or copyright, see http://ojps.aip.org/jcpo/jcpcr.jsp

can consider the molecular states "dressed" by the radiation field. The only relevant states will be the ground state with one ω_1 and one ω_2 photon, the intermediate state with an ω_2 photon, and the final state with no photons. The energies of these states are

$$E_1 = E_g + \omega_1 + \omega_2 ,$$
$$E_2 = E_e + \omega_2 , \tag{7.1}$$
$$E_3 = E_f .$$

The system is now described by the Hamiltonian Eqs. (3.1) and (4.1) with the interactions

$$V_{12} = -\mu_{eg}\epsilon_1(t)(|e\rangle\langle g| + |g\rangle\langle e|) ,$$
$$V_{23} = -\mu_{fe}\epsilon_2(t-\tau)(|f\rangle\langle g| + |g\rangle\langle f|) . \tag{7.2}$$

Here μ_{eg} and μ_{fe} are the transition dipole matrix elements. The probe absorption is given by[20]

$$\Delta\sigma(\omega_2,\omega_1) = 2\omega_2|\mu_{fe}|^2|\mu_{eg}|^2[\sigma_{\rm I} + \sigma_{\rm II}] . \tag{7.3}$$

In a stationary [continuous wave (cw)] pump–probe spectroscopy $\epsilon_1(t) = \epsilon_1$ and $\epsilon_1(t-\tau) = \epsilon_1$ independent on time. $\sigma_{\rm I}$ and $\sigma_{\rm II}$ are then given by

$$\sigma_{\rm I} = |\epsilon_1|^2|\epsilon_2|^2\langle G_{23}(s)G_{22}(s)G_{12}(s)\rho_1\rangle_p , \quad s\to 0 , \tag{7.4a}$$
$$\sigma_{\rm II} = |\epsilon_1|^2|\epsilon_2|^2\langle G_{23}(s)G_{13}(s)G_{12}(s)\rho_1\rangle_c , \quad s\to 0 . \tag{7.4b}$$

$\sigma_{\rm I}$ is a sequential pathway whereas $\sigma_{\rm II}$ is the coherent pathway. Equations (7.4) are formally identical to Eq. (3.10c). We can then use the expressions derived in this article together with Eq. (7.1) to obtain the cw absorption spectrum. Ultrafast (femtosecond) pump–probe measurements offer a much better probe of molecular and solvation dynamics. The signal is then given by the same coherent and population pathways, but with the pulse envelopes properly incorporated. Using the formal expressions developed in Ref. 20 and the correlation functions calculated in this article, we get for a time-resolved pump–probe measurement

$$\sigma_{\rm I} = (2\pi)^2\int_0^\infty dt\,\Phi(t-\tau)\frac{1}{2\pi\Delta_{12}\Delta_{23}}\frac{1}{\sqrt{1-c^2(t)}} \times\exp\left\{-q_2^2 - \frac{[q_1+q_2c(t)]^2}{1-c^2(t)}\right\}\exp(-\Gamma t) , \tag{7.5}$$

where

$$q_1 = \frac{\Delta E^{\rm I}_{23}(t)}{\sqrt{2}\Delta_{23}} , \tag{7.6a}$$

$$q_2 = \frac{\Delta E^{\rm I}_{12}}{\sqrt{2}\Delta_{12}} , \tag{7.6b}$$

$$c(t) = \frac{\langle\exp(iH_Bt)U_{23}\exp(-iH_Bt)U_{21}\rho_B\rangle}{\Delta_{12}\Delta_{23}} \tag{7.6c}$$

$$\Phi(t) = \int|\epsilon_1(t)|^2|\epsilon_2(t-\tau)|^2\,dt , \tag{7.6d}$$

$$\Delta E^{\rm I}_{23}(t) = E_{23} + \langle\exp(iH_2t)U_{23}\exp(-iH_2t)\rho_1\rangle , \tag{7.6e}$$

$$\sigma_{\rm II} = 2\pi\Phi(\tau)[R_{13}S_{13}(\Delta E^{\rm I}_{13})I(\eta^{\rm I}_{13}) - R_{12}S_{12}(\Delta E^{\rm I}_{12})I(\eta^{\rm I}_{12}) - R_{23}S_{23}(\Delta E^{\rm I}_{23})I(\eta^{\rm I}_{23})] . \tag{7.7}$$

ΔE^n_{jk}, Δ_{jk}, η^n_{jk}, and R_{jk} are defined in Eqs. (4.7), (4.8), (4.11a), and (4.11b), respectively. Γ is the inverse lifetime of level $|e\rangle$. In the high-temperature limit ΔE^n_{jk} is related to ΔG^0_{jk} and λ_{jk} by Eqs. (4.10). In a cw experiment we simply set $\Phi(\tau) = |\epsilon_1|^2|\epsilon_2|^2$ independent on time. When the frequencies ω_1 and ω_2 are tuned such that E_2 is far from E_1 and E_3, the coherent term [Eq. (7.4b)] becomes dominant and the process is direct (tunneling-like). For a given detuning, if the dephasing rate is increased the sequential term [Eq. (7.4a)] becomes dominant. Extra narrow resonances in cw pump–probe spectroscopy related to the coherent term $\sigma_{\rm II}$ have been observed.[33] In an ideal time-resolved pump–probe measurement where the two pulses are well separated in time, the coherent term vanishes and the process is sequential. This is shown by the $\Phi(\tau)$ factor in Eq. (7.7). Otherwise, the coherent term is responsible for ultrafast transients, the "coherent artifact."[33]

The present analysis shows the strikingly close resemblance between the dynamics of nonlinear optical processes and electron transfer. Since optical measurements are much more precise and detailed than kinetic measurements, one can use the present formalism to extract information from optical measurements and predict electron transfer rates in the same medium.[17(b)]

ACKNOWLEDGMENTS

The support of the Center for Photoinduced Charge Transfer sponsored by the National Science Foundation, the Office of Naval Research, and the Petroleum Research Fund, administered by the American Chemical Society, is gratefully acknowledged.

APPENDIX A: THE POPULATION PATHWAY

Using the same method used in Appendix D of Ref. 12a, we define

$$W(x,t,y) \equiv \langle\delta(x-H_{j'})G_{kk}(t)\delta(y-H_{nm})\rho_r\rangle = \frac{1}{2\pi\Delta_{j'}\Delta_{nm}}\frac{1}{\sqrt{1-c^2(t)}} \times\exp\left\{-q_2^2 - \frac{[q_1+q_2c(t)]^2}{1-c^2(t)}\right\} , \tag{A1}$$

where

$$q_1 = \frac{x-\Delta E^r_{j'}(t)}{\sqrt{2}\Delta_{j'}} , \tag{A2a}$$

$$q_2 = \frac{y-\Delta E^r_{nm}}{\sqrt{2}\Delta_{nm}} , \tag{A2b}$$

$$c(t) = \frac{\langle\exp(iH_Bt)U_{j'}\exp(-iH_Bt)U_{mn}\rho_B\rangle}{\Delta_{j'}\Delta_{nm}} , \tag{A2c}$$

$$\Delta E^r_{j'}(t) \equiv E_{j'} + \langle\exp(iH_kt)U_{j'}\exp(-iH_kt)\rho_r\rangle , \tag{A2d}$$

Downloaded 21 Jun 2002 to 128.151.176.185. Redistribution subject to AIP license or copyright, see http://ojps.aip.org/jcpo/jcpcr.jsp

where ΔE^r_{nm} and Δ_{nm} are defined previously in Eqs. (4.7) and (4.8). The time-dependent vertical transition energy $\Delta E^r_{j'}(t)$ can be written as

$$\Delta E^r_{j'}(t) \equiv E_{j'} + \langle U_{j'}\rho(t)\rangle \tag{A3a}$$

with

$$\rho(t) = \exp(-iH_k t)\rho_r \exp(iH_k t)\,. \tag{A3b}$$

We have $\rho(t) = \rho_r$ at $t = 0$ and we expect that $\rho(t) \to \rho_k$ as $t \to \infty$. $\Delta E^r_{j'}(t)$ should satisfy the following conditions

$$\Delta E^r_{j'}(0) = \Delta E^r_{j'}\,, \tag{A4a}$$

$$\Delta E^r_{j'}(\infty) = \Delta E^k_{j'}\,. \tag{A4b}$$

We shall assume that the time dependent vertical transition energy $\Delta E^r_{j'}(t)$ can be written in the form

$$\Delta E^r_{j'}(t) = \Delta E^k_{j'} - \beta\langle U_{j'}(t)U_{rk}\rho_B\rangle\,. \tag{A5}$$

Equation (A5) is exact for a harmonic solvation coordinate and it satisfies conditions (A4). Substituting Eq. (A5) into Eq. (A2a) and using the fact that the r and k in Eqs. (3.10), only assume the values of either $r = k$ or $r = n$ and $k = m$. Equation (A1) then becomes

$$W(x,t,y) = \frac{1}{2\pi\Delta_{j'}\Delta_{nm}}\frac{1}{\sqrt{1-c^2(t)}}\exp\Big[-p_1^2 - p_2^2 - \frac{2p_1p_3c(t) + (p_1^2+p_3^2)c^2(t)}{1-c^2(t)}\Big] \tag{A6}$$

with

$$p_1 = \frac{x - \Delta E^k_{j'}}{\sqrt{2}\Delta_{j'}}\,,\quad p_2 = \frac{y - \Delta E^r_{nm}}{\sqrt{2}\Delta_{nm}}\,,\quad p_3 = \frac{y - \Delta E^k_{nm}}{\sqrt{2}\Delta_{nm}}\,.$$

Inserting Eq. (A6) into Eq. (4.5b) we obtain the final expression for the frequency dependent population Green function

$$\langle G_{j'}(s)G_{kk}(s)G_{nm}(s)\rho_r\rangle_p = (2\pi)^2\int_0^\infty dt\, e^{-st}\int_{-\infty}^{\infty}dx\,dy\,\frac{s/\pi}{s^2+x^2}\frac{s/\pi}{s^2+y^2}\times[W(x,t,y) - W(x,\infty,y)]\,. \tag{A7a}$$

We can also show using Eq. (4.5a) that

$$2\,\mathrm{Re}\langle G_{nm}(s)\rho_r\rangle = 2\pi\int_{-\infty}^{\infty}dx\,\frac{s/\pi}{s^2+x^2}S_{nm}(x + \Delta E^r_{nm})\,. \tag{A7b}$$

In the limit $s \to 0$, Eqs. (A7) reduce to

$$\langle G_{j'}(s)G_{kk}(s)G_{nm}(s)\rho_r\rangle = \Big(\frac{2\pi}{\hbar}\Big)^2 S_{j'}(\Delta E^k_{j'})S_{nm}(\Delta E^r_{nm})\int_0^\infty dt\,\frac{1}{\sqrt{1-c^2(t)}} \times\exp\Big[-\frac{2q^k_{j'}q^k_{nm}c(t) - [(q^k_{j'})^2 + (q^k_{nm})^2]c^2(t)}{1-c^2(t)}\Big]\,, \tag{A8a}$$

and

$$2\,\mathrm{Re}\,\langle G_{nm}(s)\rho_r\rangle = \frac{2\pi}{\hbar}S_{nm}(\Delta E^r_{nm})\quad s\to 0\,, \tag{A8b}$$

where $q^k_{nm} = (\Delta E^k_{nm})/(\sqrt{2}\Delta_{nm})$ and $S_{nm}(x)$ is defined in Eq. (4.14). Equations (A8) were used in the rate expression [Eqs. (4.12)].

APPENDIX B: THE COHERENT PATHWAY

The coherent pathways appearing in Eqs. (3.10) can be classified into the following two types: $\langle G_{jk}(s)G_{jm}(s)G_{km}(s)\rho_r\rangle_c$ and $\langle G_{jk}(s)G_{jm}(s)G_{jk}(s)\rho_r\rangle_c$, we shall thus evaluate these two types of terms in this appendix. The same method may be applied to evaluate the more general form of the coherent pathway [Eq. (4.5c)]. We start with the coherent pathway $\langle G_{jk}(s)G_{jm}(s)G_{km}(s)\rho_r\rangle_c$. Making use of the cumulant expansion in Eq. (4.5c), we obtain

$$\langle G_{jk}(s)G_{jm}(s)G_{km}(s)\rho_r\rangle_c = 2\,\mathrm{Re}\int_0^\infty dt_3\int_0^\infty dt_2\int_0^\infty dt_1\exp[-(s+iE^r_{jk})t_3 - (s+iE^r_{jm})t_2 - (s+iE^r_{km})t_1] \times\exp\Big\{-\frac{1}{2}[\Delta^2_{jk}(t_2+t_3)^2 + \Delta^2_{km}(t_1+t_2)^2 + 2\langle U_{jk}U_{km}\rho_B\rangle(t_1+t_2)(t_2+t_3)]\Big\}\,, \tag{B1}$$

where we have used the relation $U_{jm} = U_{jk} + U_{km}$. Using the correlation coefficient γ [Eq. (4.11c)] we can recast Eq. (B1) in the form

$$\langle G_{jk}(s)G_{jm}(s)G_{km}(s)\rho_r\rangle_c = 2\,\mathrm{Re}\int_0^\infty dt_3\int_0^\infty dt_2\int_0^\infty dt_1\exp[-(s+iE^r_{jk})t_3 - (s+iE^r_{jm})t_2 - (s+iE^r_{km})t_1] \times\exp\Big\{-\frac{1+\gamma}{4}[\Delta_{jk}t_3 + (\Delta_{jk}+\Delta_{km})t_2 + \Delta_{km}t_1]^2\Big\}\exp\Big\{-\frac{1-\gamma}{4}[\Delta_{jk}t_3 + (\Delta_{jk}-\Delta_{km})t_2 - \Delta_{km}t_1]^2\Big\}\,. \tag{B2}$$

Downloaded 21 Jun 2002 to 128.151.176.185. Redistribution subject to AIP license or copyright, see http://ojps.aip.org/jcpo/jcpcr.jsp

We shall limit our discussion to the case $|\gamma|<1$. $|\gamma|=1$ will be discussed in Appendix E. By using the identity

$$\exp\left[-\frac{1}{2}\Delta^2 t^2\right]=\frac{1}{\sqrt{2\pi\Delta^2}}\int_{-\infty}^{\infty}\exp\left[-\frac{x^2}{2\Delta^2}-ixt\right]dx\,. \tag{B3}$$

Equation (B2) becomes

$$\begin{aligned}\langle G_{jk}(s)G_{jm}(s)G_{km}(s)\rho_r\rangle_c&=\frac{2}{\pi\sqrt{1-\gamma^2}}\mathrm{Re}\int_{-\infty}^{\infty}dx\int_{-\infty}^{\infty}dy\int_0^{\infty}dt_3\int_0^{\infty}dt_2\int_0^{\infty}dt_1\\&\times\exp\left(-\frac{x^2}{1+\gamma}-\frac{y^2}{1-\gamma}\right)\\&\times\exp[-(s+iA)t_3-(s+iB)t_2-(s+iC)t_1]\end{aligned} \tag{B4}$$

with

$$A=\Delta E^r_{jk}+\Delta_{jk}(x+y)\,, \tag{B5a}$$

$$B=\Delta E^r_{jm}+\Delta_{jk}(x+y)+\Delta_{km}(x-y)\,, \tag{B5b}$$

$$C=\Delta E^r_{km}+\Delta_{km}(x-y)\,. \tag{B5c}$$

The integrations over t_1, t_2, and t_3 may now be performed resulting in

$$\begin{aligned}\langle G_{jk}(s)G_{jm}(s)G_{km}(s)\rho_r\rangle_c&=\frac{2}{\pi\sqrt{1-\gamma^2}}\int_{-\infty}^{\infty}dx\int_{-\infty}^{\infty}dy\exp\left(-\frac{x^2}{1+\gamma}-\frac{y^2}{1-\gamma}\right)\\&\times\left[\frac{s}{s^2+A^2}\frac{s^2-BC}{(s^2+B^2)(s^2+C^2)}+\frac{s}{s^2+C^2}\frac{s^2-AB}{(s^2+A^2)(s^2+B^2)}-\frac{s}{s^2+B^2}\frac{-s^2+AC}{(s^2+A^2)(s^2+C^2)}\right]\equiv I_1+I_2-I_3\,.\end{aligned} \tag{B6}$$

Each of the three terms in the bracket remain finite as $s\to 0$ when the integrations are carried out. Since the three terms in the square bracket in Eq. (B6) have the similar structure, we shall evaluate the first term (i.e., I_1) in detail. I_2 and I_3 can be evaluated in a similar way. We introduce the variable

$$z=\Delta E^r_{jk}+\Delta_{jk}(x+y)\,, \tag{B7}$$

we then have

$$\begin{aligned}I_1=\int_{-\infty}^{\infty}dz\frac{s/\pi}{s^2+z^2}\frac{2}{\Delta_{jk}\sqrt{1-\gamma^2}}\int_{-\infty}^{\infty}dy&\times\exp\left\{-\frac{[(z-\Delta E^r_{jk})/\Delta_{jk}+y]^2}{1+\gamma}-\frac{y^2}{1-\gamma}\right\}\\&\times\frac{s^2-(z+f+2y\Delta_{km})(f+2y\Delta_{km})}{[s^2+(z+f+2y\Delta_{km})^2][s^2+(f+2y\Delta_{km})^2]}\end{aligned} \tag{B8}$$

with

$$f=\Delta E^r_{km}-\frac{\Delta_{km}}{\Delta_{jk}}\Delta E^r_{jk}+\frac{\Delta_{km}}{\Delta_{jk}}z\,. \tag{B9}$$

In deriving Eq. (B8) we have repeatedly used the relation $\Delta E^r_{jm}=\Delta E^r_{jk}+\Delta E^r_{km}$. Making use of the following identity (see Appendix C):

$$\begin{aligned}\frac{1}{\sqrt{2\pi\Delta^2}}\int_{-\infty}^{\infty}dy\exp\left(-\frac{y^2}{2\Delta^2}\right)&\times\frac{s^2-(a_1+y)(a_2+y)}{[s^2+(a_1+y)^2][s^2+(a_2+y)^2]}\\&=\int_0^{\infty}dx\frac{\sin[(a_1-a_2)x/2]}{(a_1-a_2)/2}\\&\times\cos\left(\frac{a_1+a_2}{2}x\right)\exp\left(-sx-\frac{1}{2}\Delta^2x^2\right),\end{aligned} \tag{B10}$$

we get

$$I_1=\int_{-\infty}^{\infty}dz\frac{s/\pi}{s^2+z^2}[-I^r_{jk}(z,s)]\,, \tag{B11}$$

$$\begin{aligned}I^r_{jk}(z,s)=&-2\pi\frac{1}{\sqrt{4\pi k_B T\lambda_{jk}}}\exp\left[-\frac{(z-\Delta E^r_{jk})^2}{4k_BT\lambda_{jk}}\right]\\&\times\int_0^{\infty}dx\frac{\sin(zx/2)}{z/2}\\&\times\cos\left\{\left[\left(\frac{1}{2}-\frac{\lambda_2}{\lambda_{jk}}\right)z+\frac{\eta^r_{jk}}{\sqrt{R_{jk}}}\right]x\right\}\\&\times\exp\left(-sx-\frac{x^2}{2R_{jk}}\right).\end{aligned} \tag{B12}$$

The parameters λ_2, λ_{jk}, η^r_{jk} and R_{jk} are defined in Eq. (4.8)–(4.11). Applying a similar method to I_2, I_3 and to the other coherent pathway $\langle G_{jk}(s)G_{jm}(s)G_{km}(s)\rho_r\rangle_c$, we finally obtain from the coherent correlation function

$$\langle G_{jk}(s)G_{jm}(s)G_{km}(s)\rho_r\rangle_c=\int_{-\infty}^{\infty}dz\frac{s/\pi}{s^2+z^2}[I^r_{jm}(z,s)-I^r_{jk}(z,s)-I^r_{km}(z,s)] \tag{B13a}$$

and

$$\langle G_{jk}(s)G_{jm}(s)G_{kj}(s)\rho_r\rangle_c=\int_{-\infty}^{\infty}dz\frac{s/\pi}{s^2+z^2}[-I^r_{jm}(z,s)]\,. \tag{B13b}$$

In the limits $s\to 0$, Eqs. (B13) reduce to

$\langle G_{jk}(s)G_{jm}(s)G_{km}(s)\rho_r\rangle_c$

Downloaded 21 Jun 2002 to 128.151.176.185. Redistribution subject to AIP license or copyright, see http://ojps.aip.org/jcpo/jcpcr.jsp

$$= \frac{2\pi}{\hbar}\left[R_{jm}S_{jm}(\Delta E^r_{jm})I(\eta^r_{jm}) - R_{jk}S_{jk}(\Delta E^r_{jk})I(\eta^r_{jk}) - R_{km}S_{km}(\Delta E^r_{km})I(\eta^r_{km})\right], \quad \text{(B14a)}$$

$$\langle G_{jk}(s)G_{jm}(s)G_{jk}(s)\rho_r\rangle|_{s\to 0} = -\frac{2\pi}{\hbar}R_{jm}S_{jm}(\Delta E^r_{jm})I(\eta^r_{jm}). \quad \text{(B14b)}$$

It should be pointed out that Eqs. (B14) can be alternatively derived from Eq. (B4) by sending $s\to 0$ first, then taking the real part of the integrand and using the relation

$$\cos(a+b+c) = \cos a\cos(b+c) + \cos c\cos(a+b) - \cos b\cos(a-c). \quad \text{(B15)}$$

Equations (B14) were used in our final rate expression [Eq. (4.12)].

APPENDIX C: DERIVATION OF EQ. (B10)

Using the following integral:

$$\frac{s^2-(a_1+y)(a_2+y)}{[s^2+(a_1+y)^2][s^2+(a_2+y)^2]} = \mathrm{Re}\int_0^\infty dt_1\int_0^\infty dt_2 \exp\{[s+i(a_1+y)]t_1 - [s+i(a_2+y)]t_2\}, \quad \text{(C1)}$$

the left-hand side of the Eq. (B10) becomes

$$\frac{1}{2\pi\Delta^2}\mathrm{Re}\int_{-\infty}^\infty dy\int_0^\infty dt_1\int_0^\infty dt_2 \exp\left(-\frac{y^2}{2\Delta^2} - \{[s+i(a_1+y)]t_1 - [s+i(a_2+y)]t_2\}\right)$$
$$= \mathrm{Re}\int_0^\infty dt_1\int_0^\infty dt_2 \exp[-(s+ia_1)t_1 - (s+ia_2)t_2 - \tfrac{1}{2}\Delta^2(t_1+t_2)^2]. \quad \text{(C2)}$$

Making the substitutions $x = t_1 + t_3$ and $t = t_1$, we get

$$\mathrm{Re}\int_0^\infty dt\int_t^\infty dx \exp[-i(a_1-a_2)t - ia_2x - sx - \tfrac{1}{2}\Delta^2x^2]$$
$$= \mathrm{Re}\int_0^\infty dx\int_0^x dt \exp[-i(a_1-a_2)t - ia_2x - sx - \tfrac{1}{2}\Delta^2x^2] = \int_0^\infty dx\frac{1}{a_1-a_2}(\sin a_1x - \sin a_2x)\times\exp(-sx-\tfrac{1}{2}\Delta^2x^2) \quad \text{(C3)}$$

which proves Eq. (B10).

APPENDIX D: DERIVATION OF EQ. (4.10)

In the high-temperature limit, we may use the expansion

$$\exp[-\beta(H_B+U_j)] = \exp(-\beta H_B) - \beta\exp(-\beta H_B)U_j + (\beta^2/2)\exp(-\beta H_B)U_j^2. \quad \text{(D1)}$$

The average energy when the system is in the $|j\rangle$ state is given by

$$G^0_j \equiv \langle H_j\rho_j\rangle = E_j + \langle H_B\rho_j\rangle + \langle U_j\rho_j\rangle. \quad \text{(D2)}$$

We further note that

$$\rho_j = \frac{\exp[-\beta(H_B+U_j)]}{\langle\exp[-\beta(H_B+U_j)]\rangle}. \quad \text{(D3)}$$

Inserting Eqs. (D1) and (D3) into Eq. (D2), and truncating the expansion to second order in U_j, we obtain

$$G^0_j = E_j + \langle H_B\rho_B\rangle - \beta\langle U_j^2\rho_B\rangle - (\beta^2/2)\langle H_B\rho_B\rangle\langle U_n^2\rho_B\rangle + (\beta^2/2)\langle U_n^2H_B\rho_B\rangle. \quad \text{(D4)}$$

By using the following relation:

$$\frac{\partial}{\partial\beta}\langle U_n^2\rho_B\rangle = -\langle U_n^2H_B\rho_B\rangle + \langle U_n^2\rho_B\rangle\langle H_B\rho_B\rangle, \quad \text{(D5)}$$

Eq. (D4) reduces to

$$G^0_j = E_n + \langle H_B\rho_B\rangle - \beta\langle U_j^2\rho_B\rangle - \frac{\beta^2}{2}\frac{\partial}{\partial\beta}\langle U_n^2\rho_B\rangle. \quad \text{(D6)}$$

Since $\langle U_n^2\rho_B\rangle$ is linearly proportional to k_BT,[12(a)] we define

$$\langle U_n^2\rho_B\rangle = (\lambda/\beta). \quad \text{(D7)}$$

Substituting Eq. (D7) into Eq. (D6) we finally obtain

$$G^0_j = E_j + \langle H_B\rho_B\rangle - (\beta/2)\langle U_j^2\rho_B\rangle, \quad \text{(D8)}$$

$$\Delta G^0_{jk} \equiv G^0_j - G^0_k = E_j - E_k - (\beta/2)\langle U_j^2\rho_B\rangle + (\beta/2)\langle U_k^2\rho_B\rangle. \quad \text{(D9)}$$

We further have

$$\Delta E^m_{jn} \equiv \langle(H_j - H_n)\rho_m\rangle = E_j - E_n - \beta\langle U_{jn}U_m\rho_B\rangle. \quad \text{(D10)}$$

Equations (4.10) immediately follow by combining Eqs. (D9), (D10), (4.7), and (4.8).

APPENDIX E: A SINGLE SOLVATION COORDINATE AND A GENERALIZED ZUSMAN'S EQUATION

In this appendix we consider the special case whereby the solvent fluctuations on the various sites are fully correlated, i.e., $|\gamma| = 1$. In this case, we get from Eq. (4.11c)

$$\langle U_{jk}U_{km}\rho_B\rangle = \pm[\langle U_{jk}^2\rho_B\rangle\langle U_{km}^2\rho_B\rangle]^{1/2}. \quad \text{(E1)}$$

A physical realization of this situation is when the charge distribution of the electron transfer system is well localized. The solvent polar molecules experience the dipolar field created by the charge transfer system. The strength of the dipolar field will be different when the electron is at different sites so that the fields can be written as

$$\mathbf{D}_j(\mathbf{r}) = D_j\boldsymbol{\phi}(\mathbf{r}), \quad j = 1,2,3. \quad \text{(E2)}$$

Here $\boldsymbol{\phi}_j(\mathbf{r})$ is the electrostatic field created by a dipole. The corresponding interaction energy can be simplified as

Downloaded 21 Jun 2002 to 128.151.176.185. Redistribution subject to AIP license or copyright, see http://ojps.aip.org/jcpo/jcpcr.jsp

$$U_j = D_j U, \quad U = -\int \mathbf{P}(\mathbf{r})\phi(\mathbf{r})\, d\mathbf{r}. \tag{E3}$$

Thus, U is the only relevant solvent coordinate in the problem. Equation (E3) is a sufficient condition for Eq. (E1) to hold. When $|\gamma| = 1$, both R_{jk} and η^r_{jk} [Eqs. (4.11)] diverge. Using Eq. (4.22) we then get

$$R_{jk} I(\eta^r_{jk}) \cong R_{jk}/(\eta^r_{jk})^2 = \left[\frac{\lambda_{jk}}{\Delta E^r_{jm}\lambda_k + \Delta E^r_{km}\lambda_j}\right]^2. \tag{E4}$$

The rate matrix for $\gamma = \pm 1$ can thus be calculated using Eqs. (4.12) with the substitution of Eq. (E4). After some algebraic manipulations we get for K_{31} when $\gamma = 1$:

$$K_{31} = \sigma_{21}\sigma_{32}\tau_c + \frac{2\pi}{\hbar} V^2_{12} V^2_{23} \frac{1}{[\Delta E^1_{23} - \Delta E^1_{13}(\Delta_{23}/\Delta_{13})]^2} \times \left[S_{13}(\Delta E^1_{13}) - \frac{\Delta^2_{23}}{\Delta^2_{13}} S_{23}(\Delta E^1_{23}) - \frac{\Delta^2_{12}}{\Delta^2_{13}} S_{12}(\Delta E^1_{12})\right]. \tag{E5}$$

It should be pointed out that Eqs. (4.10) still hold in this case. The conventional superexchange result can be obtained by neglecting the last two terms in the square bracket of Eq. (E5).

Equations (E5) can also be obtained from a generalized Zusman's equation[10] which is the combination of the Bloch and the Smoluchowski equations. We thus write

$$\dot{\sigma}_{jj}(x,t) = (-i)\sum_l V_{lj}[\sigma_{lj}(x,t) - \sigma_{jl}(x,t)] - \Lambda_{jj}\frac{\partial}{\partial x}\left[\Delta'^2_{jj}\frac{\partial}{\partial x} + x - \lambda'_{jj}\right]\sigma_{jj}(x,t) \tag{E6a}$$

$$\dot{\sigma}_{jk}(x,t) = (-i)\sum_l [V_{lj}\sigma_{lk}(x,t) - V_{lk}\sigma_{jl}(x,t)] - \Lambda_{jk}\frac{\partial}{\partial x}\left[\Delta'^2_{jk}\frac{\partial}{\partial x} + x - \lambda'_{jk}\right]\sigma_{jk}(x,t) - i[E_{jk} + D_{jk}x]\sigma_{jk}(x,t), \quad j \neq k, \tag{E6b}$$

where

$$\Delta'_{jk} = \int \phi(\mathbf{r}_1)\phi(\mathbf{r}_2)\langle \mathbf{P}(\mathbf{r}_1)\mathbf{P}(\mathbf{r}_2)\rho_{jk}\rangle d\mathbf{r}_1 d\mathbf{r}_2,$$

$$\lambda'_{jk} = \frac{1}{k_B T}\int \phi(\mathbf{r}_1)\langle \mathbf{P}(\mathbf{r}_1)\rho_{jk}\rangle d\mathbf{r}_1,$$

$$x = U,$$

$$D_{jk} = D_j - D_k,$$

$$\rho_{jk} = \exp(-\beta H_{jk})/\langle exp(-\beta H_{jk})\rangle,$$

$$H_{jk} = (H_j + H_k)/2.$$

Λ_{jk} is a rate constant which describes how fast the system relaxes to thermal equilibrium. The population on the state $|j\rangle$ is given by

$$p_j(t) = \int_{-\infty}^{\infty} dx \sigma_{jj}(x,t).$$

By using standard projection operator techniques we can derive the generalized master equation [Eq. (2.12)] starting with Eq. (E6). The result [Eq. (E5)] follows by applying the static approximation for the coherent Green functions.

[1] *Photoinduced Electron Transfer Part A*, edited by M. A. Fox and M. Chanon, (Elsevier, Amsterdam, 1988).
[2] (a) M. W. Makinen, S. A. Schichman, S. C. Hill, and H. B. Gray, Science **222**, 929 (1983); (b) G. McLendon, Acc. Chem. Res. **21**, 160 (1988).
[3] G. L. Closs and J. R. Miller, Science **240**, 440 (1988).
[4] See papers in *The Photosynthetic Bacterial Reaction Center*, edited by J. Breton and A. Vermeglio (Plenum, New York, 1988).
[5] D. C. Mattis, *The Theory of Magnetism I* (Springer, Berlin, 1981).
[6] H. McConnel, J. Chem. Phys. **35**, 508 (1961).
[7] E. Stein and H. Taube, J. Am. Chem. Soc. **103**, 693 (1981); A. Beretan and J. J. Hopfield, *ibid.* **106**, 1584 (1984); M. Redi and J. J. Hopfield, J. Chem. Phys. **72**, 6651 (1980); J. R. Miller and J. V. Beitz, *ibid.* **74**, 6746 (1981).
[8] T. Holstein, Ann. Phys. **8**, 325 (1959); **132**, 212 (1981).
[9] (a) R. A. Marcus and N. Sutin Biochem. Biophys. Acta **811**, 275 (1985); (b) J. Jortner, *ibid.* **594**, 193 (1980).
[10] L. D. Zusman, Chem. Phys. **49**, 295 (1980); **80**, 29 (1983); L. D. Zusman and A. B. Helman, Opt. Spectrosc. **53**, 248 (1982).
[11] R. F. Loring, D. S. Franchi, and S. Mukamel, Phys. Rev. B **37**, 1874 (1988); S. Mukamel, D. S. Franchi, and R. F. Loring Chem. Phys. **128**, 99 (1988); R. F. Loring, M. Sparpaglione, and S. Mukamel, J. Chem. Phys. **86**, 2249 (1987).
[12] (a) M. Sparpaglione and S. Mukamel, J. Chem. Phys. **88**, 3263; (b) *ibid*, 4300 (1988).
[13] H. Haken and G. Strobl, Z. Phys. **262**, 135 (1973).
[14] M. Grover and R. Silbey, J. Chem. Phys. **54**, 4853 (1971).
[15] N. Bloembergen, *Nonlinear Optics* (Benjamin, New York, 1965); Y. R. Shen, *The Principles of Nonlinear Optics* (Wiley, New York, 1984).
[16] S. Mukamel, Phys. Rep. **93**, 1 (1982); Adv. Chem. Phys. **70**, 165 (1988).
[17] (a) Y. J. Yan, M. Sparpaglione, and S. Mukamel, J. Phys. Chem. **92**, 4842 (1988); (b) S. Mukamel and Y. J. Yan, Acct. Chem. Res. **22**, 301 (1989).
[18] C. H. Brito Cruz, R. L. Fork, W. Knox, and C. V. Shank, Chem. Phys. Lett. **132**, 341 (1986); P. C. Becker, R. L. Fork, C. H. Brito Cruz, J. P. Gordon, and C. V. Shank, Phys. Rev. Lett. **60**, 2462 (1988).
[19] M. Dantus, M. J. Rosker, and A. H. Zewail, J. Chem. Phys. **89**, 6113, 6128 (1988); M. J. Rosker, M. Dantus, and A. H. Zewail, Science **241**, 1200 (1988).
[20] R. F. Loring, Y. J. Yan, and S. Mukamel, J. Chem. Phys. **87**, 5840 (1987); Y. J. Yan, L. Fried, and S. Mukamel, J. Phys. Chem. (in press).
[21] R. Zwanzig, Physica **30**, 1109 (1964).
[22] A. A. Ovchinnikov and M. Y. Ovchinnikova, Sov. Phys. JETP **29**, 688 (1969).
[23] J. Ulstrup, *Theory of Electron Transfer Reactions*, (Springer, Berlin 1979).
[24] J. S. Bader and D. Chandler, Chem. Phys. Lett. **157**, 501 (1989).
[25] M. J. Lax, J. Chem. Phys. **20**, 1752 (1952).
[26] R. A. Marcus, Chem. Phys. Lett. **133**, 471 (1987); in Ref. 4, p. 389.
[27] M. Bixon, J. Jortner, M. Plato, and M. E. Michel-Beyerle, in Ref. 4, p. 399.
[28] Y. Won and R. A. Friesner, Biochem. Biophys. Acta **935**, 9 (1988).
[29] J. Breton, J. L. Martin, A Migus, A. Antonetti, and A. Orszag, Proc. Nat. Acad. Sci. USA **83**, 5121 (1986); G. R. Fleming, J. L. Martin, and J. Breton, Nature **333**, 190 (1988); W. Holzapfel, U. Finkele, W. Kaiser, D. Oesterhelt, H. Scheer, H. U. Stilz, and W. Zinth, Chem. Phys. Lett. **160**, 1–7 (1989).
[30] Y. Hu and S. Mukamel, *Perspectives in Photosynthesis*, edited by J. Jortner and B. Pullman (Kluwer Academic Publishers, The Netherlands, 1989) (in press); Chem. Phys. Lett. **160**, 410 (1989).
[31] R. Kubo, Adv. Chem. Phys. **15**, 101 (1969).
[32] Y. J. Yan and S. Mukamel, J. Chem. Phys. **89**, 5160 (1988).
[33] H. J. Eichler, D. Langhans, and F. Massmann, Opt. Comm. **50**, 117 (1984); R. W. Boyd and S. Mukamel, Phys. Rev. A **29**, 1973 (1984).

Downloaded 21 Jun 2002 to 128.151.176.185. Redistribution subject to AIP license or copyright, see http://ojps.aip.org/jcpo/jcpcr.jsp